iScience

CellPress
OPEN ACCESS

Article

TACI Constrains T_H17 Pathogenicity and Protects against Gut Inflammation

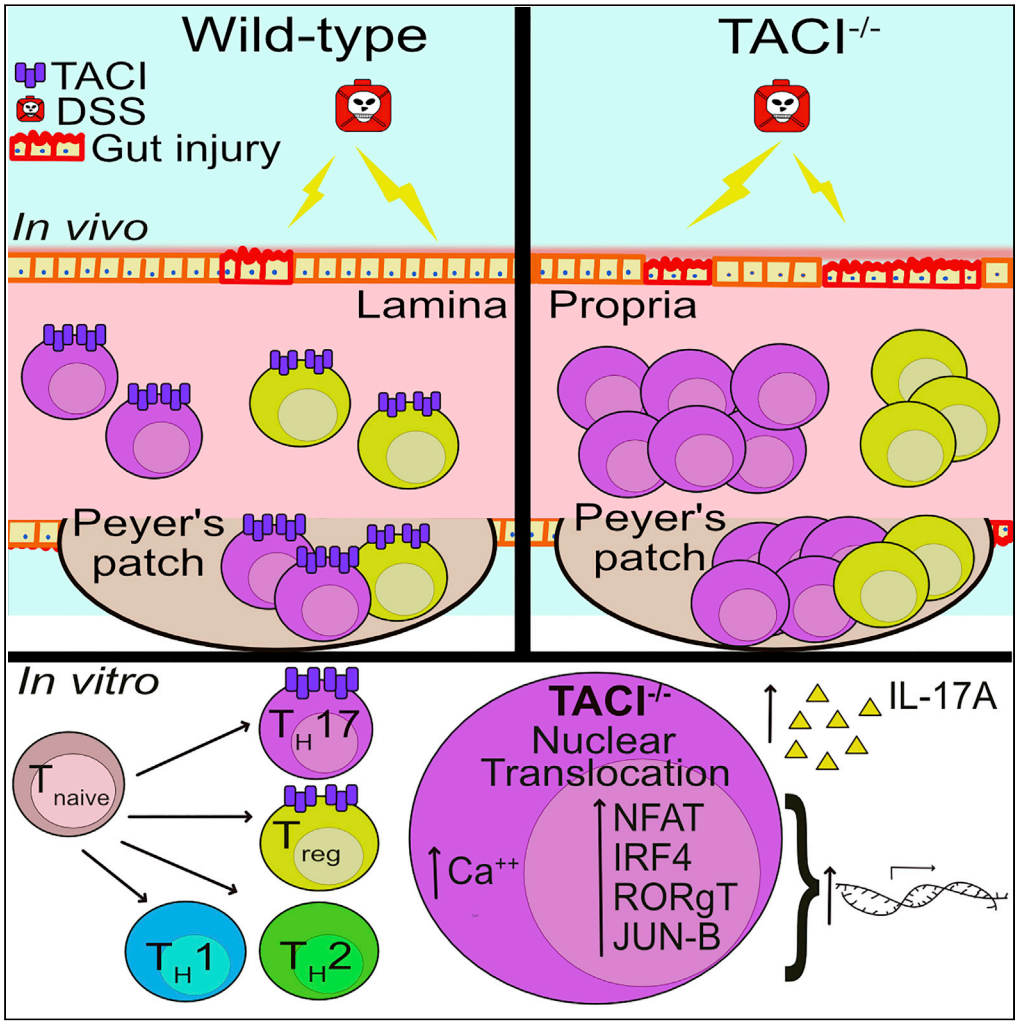

Andy Hee-Meng Tan, Gloria Hoi Wan Tso, Biyan Zhang, ..., Alison P. Lee, Shengli Xu, Kong-Peng Lam

andy_tan@bti.a-star.edu.sg (A.H.-M.T.)
lam_kong_peng@bti.a-star.edu.sg (K.-P.L.)

HIGHLIGHTS

TACI expression is induced in T_H17 but not T_H1 or T_H2 cells differentiated *in vitro*

$TACI^{-/-}$ mice have expanded T_H17 and T_{reg} populations in various organs

$TACI^{-/-}$ mice have enhanced susceptibility to intestinal disease

Activation of T_H17-promoting transcription factors is enhanced in $TACI^{-/-}$ $CD4^+$ T cells

Tan et al., iScience *23*, 101707
November 20, 2020
https://doi.org/10.1016/j.isci.2020.101707

iScience

CellPress
OPEN ACCESS

Article

TACI Constrains T_H17 Pathogenicity and Protects against Gut Inflammation

Andy Hee-Meng Tan,[1,*] Gloria Hoi Wan Tso,[1,8] Biyan Zhang,[1,8] Pei-Yun Teo,[1,8] Xijun Ou,[1,7,8] Sze-Wai Ng,[1,8] Alex Xing Fah Wong,[1] Sean Jing Xiang Tan,[1] Arleen Sanny,[1] Susana Soo-Yeon Kim,[1] Alison P. Lee,[1] Shengli Xu,[1,3] and Kong-Peng Lam[1,2,3,4,5,6,9,*]

SUMMARY

TACI (transmembrane activator and calcium modulator and cyclophilin ligand interactor) plays critical roles in B cells by promoting immunoglobulin class switching and plasma cell survival. However, its expression and function in T cells remain controversial. We show here that TACI expression can be strongly induced in murine $CD4^+$ T cells *in vitro* by cytokines responsible for T_H17 but not T_H1 or T_H2 differentiation. Frequencies and numbers of T_H17 cells were elevated in $TACI^{-/-}$ compared with wild-type mice as well as among $TACI^{-/-}$ versus wild-type $CD4^+$ T cells in mixed bone marrow chimeras, arguing for a T cell-intrinsic effect in the contribution of TACI deficiency to T_H17 cell accumulation. $TACI^{-/-}$ mice were more susceptible to severe colitis induced by dextran sodium sulfate or adoptive T cell transfer, suggesting that TACI negatively regulates T_H17 function and limits intestinal inflammation in a cell-autonomous manner. Finally, transcriptomic and biochemical analyses revealed that $TACI^{-/-}$ $CD4^+$ T cells exhibited enhanced activation of T_H17-promoting transcription factors NFAT, IRF4, c-MAF, and JUNB. Taken together, these findings reveal an important role of TACI in constraining T_H17 pathogenicity and protecting against gut disease.

INTRODUCTION

The transmembrane activator and calcium modulator and cyclophilin ligand interactor (TACI encoded by the Tnfrsf13*b* gene) is a member of the tumor necrosis factor receptor superfamily (TNFRSF) and is closely related to the B cell activating factor receptor (BAFF-R encoded by the *Tnfrsf13c* gene) and B cell maturation antigen (BCMA encoded by the *Tnfrsf17* gene) (Mackay and Schneider, 2008). TACI shares one of its binding ligands, BAFF, with BAFF-R and BCMA and the other ligand, a proliferation-inducing ligand (APRIL), with BCMA. Previous studies have shown TACI to be expressed in B cells (Rickert et al., 2011; Salzer et al., 2007), macrophages (Allman et al., 2015), and possibly also in activated T cells (Von Bülow and Bram, 1997). As expression of TACI is most prominent in B cells, most studies have focused on defining the functions of TACI in B cells, including its negative regulation of B cell expansion (Yan et al., 2001) and germinal center (GC) B cell formation (Ou et al., 2012) and promotion of plasma cell survival (Bossen et al., 2008; Ou et al., 2012) and immunoglobulin (Ig) isotype switching, diversification, and production (Figgett et al., 2015; He et al., 2010; Salzer et al., 2007; Seshasayee et al., 2003). TACI has also been shown to mediate BAFF- and APRIL-induced signals in innate immune cells that favor M1 macrophage polarization (Allman et al., 2015).

The expression of TACI in T cells is controversial, and the exact role of TACI in T cell function remains obscure, with studies reporting conflicting results (Mackay and Leung, 2006). TACI was first found to be expressed in activated mouse and human T cells using flow cytometry (Von Bülow and Bram, 1997; Wang et al., 2001). TACI expression was also observed on the surface of a small subset of $CD3^+$ T cells in synovial tissues of human patients with rheumatoid arthritis (Seyler et al., 2005). In contrast, an independent study failed to detect $TACI^+$ T cells derived from the blood and secondary lymphoid organs of mouse and human origin (Ng et al., 2004). Moreover, another study found TACI mRNA levels to be at least an order of magnitude weaker in human T cells compared with B cells, which was further decreased upon T cell activation (Wu et al., 2000). Characterization of a possible role of TACI in T cell signaling has been largely confined to

[1]Bioprocessing Technology Institute, Agency for Science, Technology and Research, 20 Biopolis Way, #06-01 Centros, Singapore 138668, Singapore

[2]Singapore Immunology Network, Agency for Science, Technology and Research, Singapore 138648, Singapore

[3]Department of Physiology, Yong Loo Lin School of Medicine, National University of Singapore, Singapore 117599, Singapore

[4]Departments of Microbiology and Immunology, Yong Loo Lin School of Medicine, National University of Singapore, Singapore 117599, Singapore

[5]Departments of Pediatrics, Yong Loo Lin School of Medicine, National University of Singapore, Singapore 117599, Singapore

[6]School of Biological Sciences, Nanyang Technological University, Singapore 639798, Singapore

[7]Present address: Department of Biology, Southern University of Science and Technology, 1088 Xueyuan Blvd., Nanshan District, Shenzhen, Guangdong, China 518055, China

[8]These authors contributed equally

[9]Lead Contact

*Correspondence: andy_tan@bti.a-star.edu.sg (A.H.-M.T.), lam_kong_peng@bti.a-star.edu.sg (K.-P.L.)

https://doi.org/10.1016/j.isci.2020.101707

transiently over-expressing TACI in Jurkat T cells and cross-linking the receptor with TACI-specific antibodies (Abs). Such an inquiry showed that TACI activates the transcription factors nuclear factor of activated T cells (NFAT), nuclear factor κ-light-chain-enhancer of activated B cells (NF-κB) and activator protein (AP)-1 (Von Bülow and Bram, 1997). However, the physiological role of TACI in T cells remains unaddressed.

In this study, we sought to clarify the role of TACI, if any, in T cell function and differentiation. We found TACI expression to be strongly induced in $CD3^+CD4^+$ T cells by TGF-β and further enhanced by IL-6 but not IL-2. TACI-deficient ($TACI^{-/-}$) T cells were shown to exhibit enhanced activation of the transcription factors NFAT, interferon regulatory factor 4 (IRF4), Musculo Aponeurotic Fibrosarcoma oncogene (c-MAF), and JunB proto-oncogene (JUNB), which are known to be important for the differentiation of IL-17-producing T helper (T_H17) cells. Accordingly, we found the frequencies and numbers of T_H17 cells in the various lymphoid organs to be higher in $TACI^{-/-}$ compared with wild-type (WT) mice. Similar expansion of T_H17 cells observed among $TACI^{-/-}$ versus WT $CD4^+$ T cells in competitive chimeras that were reconstituted with equal ratio of WT and $TACI^{-/-}$ bone marrow cells suggested a cell-intrinsic effect of TACI in constraining T_H17 accumulation. Furthermore, the induction of experimental colitis with dextran sodium sulfate (DSS) led to more severe colitis in $TACI^{-/-}$ compared with WT mice, as did the transfer of naive $TACI^{-/-}$ versus WT T cells into immune-deficient $RAG1^{-/-}$ mice. Collectively, our findings reveal for the first time a unique physiological role of TACI in limiting T_H17 cell activation and pathogenicity, possibly to maintain gut homeostasis.

RESULTS

TACI Expression in $CD4^+$ T Cells Is Induced by TGF-β and Further Enhanced by IL-6 but Not IL-2

Previous data have shown that TACI expression in T cells can be induced by phorbol-12-myristate-13-acetate (PMA) and ionomycin treatment (Von Bülow and Bram, 1997). We sought to ascertain if TCR-mediated activation signals, in combination with those triggered by cytokines, could more readily induce TACI expression in $CD3^+CD4^+$ T cells. We stimulated $CD4^+$ T cells isolated from the spleens (Spl) of WT mice with anti-CD3 and anti-CD28 Abs and various combinations of cytokines known to promote T helper 1 (T_H1), T helper 2 (T_H2), T helper 17 (T_H17), or T regulatory (T_{reg}) cell differentiation and assessed the level of TACI expression in these polarized cells, with $TACI^{-/-}$ $CD4^+$ T cells cultured under corresponding conditions used as negative controls. Activation of $CD4^+$ T cells by anti-CD3 and anti-CD28 Abs in non-polarizing (T_H0; anti-IFN-γ + anti-IL-4 Abs), T_H1-polarizing (IL-12 + anti-IL-4 Ab), or T_H2-polarizing (IL-4 + anti-IFN-γ Ab) conditions failed to induce TACI cell surface protein (Figures 1A and 1B) and mRNA (Figure 1C) expression. Strikingly, cytokines promoting T_H17 (TGF-β + IL-6 + IL-23) or T_{reg} (TGF-β + IL-2) differentiation strongly upregulated TACI protein and mRNA expression, with T_H17-promoting cytokines eliciting the most significant increase. In contrast, expression of the closely related TNFRSF members BAFF-R and BCMA were similar in WT and $TACI^{-/-}$ $CD4^+$ T cells stimulated under various polarizing conditions, with that of BAFF-R being modestly increased versus isotype control in both WT and $TACI^{-/-}$ T_H17 and T_{reg} cells (Figure S1). These data suggest that cytokine combinations driving T_H17 and T_{reg} lineage commitment specifically induced TACI but not BAFF-R or BCMA expression in these lineages.

To determine the relative contributions of the cytokines involved in T_H17 and T_{reg} differentiation in eliciting TACI expression, we incubated anti-CD3-and anti-CD28-activated $CD4^+$ T cells with individual or specific combinations of cytokines and examined their cell surface expression of TACI (Figures 1D and 1E). We found TGF-β, but not IL-6, IL-23, or combination of the latter two, to robustly upregulate TACI expression (27.7% versus < 1% $TACI^+$ cells induced by TGF-β versus IL-6, IL-23 or IL-6 + IL-23). Interestingly, IL-6, but not IL-23, when administered together with TGF-β, further enhanced TACI expression (47.0% versus 27.0% $TACI^+$ cells induced by TGF-β + IL-6 versus TGF-β + IL-23) on activated $CD4^+$ T cells (Figure 1D). We also examined if IL-2 supplementation could further enhance TGF-β-induced TACI expression on activated $CD4^+$ T cells and found no such effect (Figure 1E). Taken together, our findings define a previously unappreciated role for cytokines, specifically TGF-β that promotes T_H17 and T_{reg} development, in inducing TACI expression in $CD4^+$ T cells.

TACI Limits IL-17A Production by *In Vitro* Differentiated T_H17 Cells

We next asked whether specific upregulation of TACI expression in T_H17 and T_{reg} but not T_H1 and T_H2 cells correlated with an important role for TACI in modulating the *in vitro* differentiation of T_H17 and T_{reg} but not T_H1 and T_H2 cells. To this end, we activated WT and $TACI^{-/-}$ $CD4^+$ T cells under various polarizing

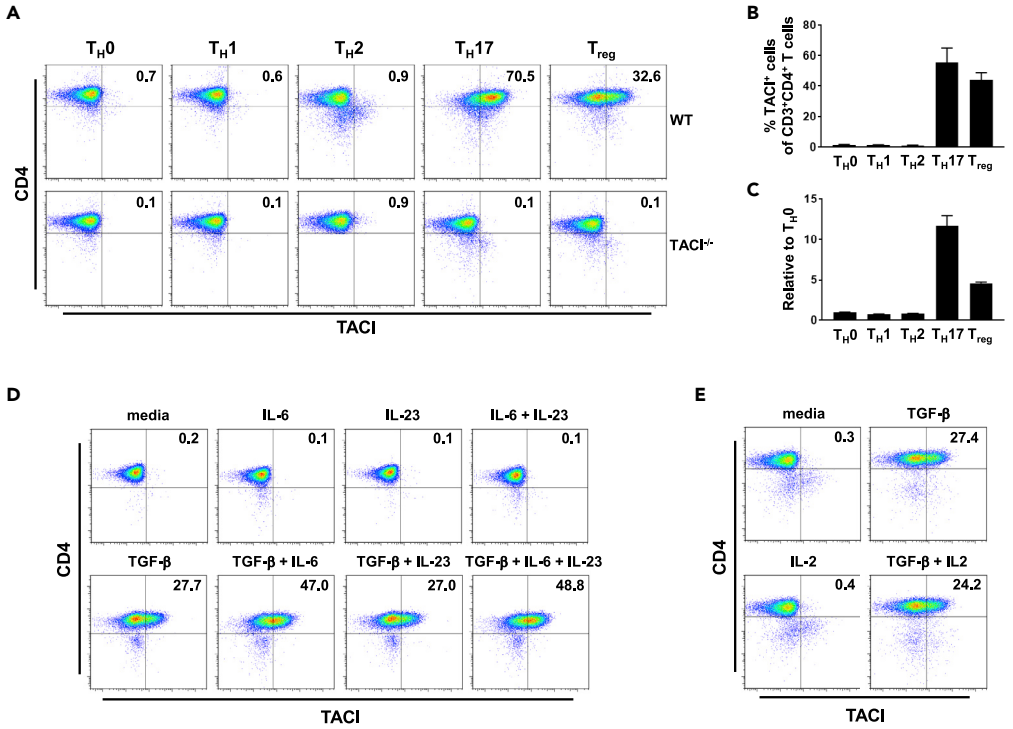

Figure 1. Induction by TGF-β and Enhancement by IL-6 of TACI Expression in $CD3^+CD4^+$ T Cells

(A and B)Cell surface expression of TACI in $CD3^+CD4^+$ T cells isolated from Spl of WT and $TACI^{-/-}$ mice (A), or WT mice only (B), stimulated under T_H0-, T_H1-, T_H2-, T_H17-, or T_{reg}-polarizing conditions for 3 days and assessed by flow cytometry.

(C) Transcript levels of TACI in WT $CD3^+CD4^+$ T cells stimulated as in (A) and assessed by quantitative real-time PCR. Transcript levels in T_H1, T_H2, T_H17, or T_{reg} cells were normalized to that in T_H0 cells.

(D and E) Cell surface expression of TACI in WT $CD3^+CD4^+$ T cells activated with anti-CD3 and anti-CD28 Abs in the presence of indicated cytokines for 3 days.

Data in (A), (D), and (E) are representative of three independent experiments. Data in (B) and (C) are the mean ± SEM of three independent experiments.

conditions for 3 days as shown in Figure 1 and assessed their production of signature cytokines or expression of Foxp3. We confirmed that *in vitro* differentiated WT and $TACI^{-/-}$ T_H1 cells produced high but comparable concentrations of IFN-γ (Figure S2A). IL-4 production by WT and $TACI^{-/-}$ T_H1 cells was undetectable as expected (Figure S2B). WT and $TACI^{-/-}$ T_H2 cells, on the other hand, produced expectedly high but indistinguishable concentrations of IL-4 (Figure S2B). Both produced low levels of IFN-γ (Figure S2A). In contrast, $TACI^{-/-}$ T_H17 cells produced significantly higher concentration of IL-17A compared with their WT counterparts, although WT and $TACI^{-/-}$ $CD4^+$ T cells differentiated under T_{reg}-polarizing conditions yielded similar frequencies of $Foxp3^+$ cells (Figure S2D).

To ascertain if the modulation of T_H17 differentiation by TACI is dependent on its binding of ligands, we added increasing concentrations (1, 10, or 100 ng/mL) of recombinant BAFF or APRIL to WT $CD4^+$ T cells differentiated under T_H17- or T_{reg}-polarizing conditions (Figure S3B) and found neither BAFF nor APRIL reduced the frequencies of T_H17 ($IL\text{-}17A^+$; top panel) or T_{reg} ($Foxp3^+$; bottom panel) cells after 3 days in culture compared with vehicle control regardless of the concentration of ligand employed. This was not due to lack of functional potency of the ligands since, consistent with the well-known role of these ligands to co-stimulate B cell responses, each ligand enhanced proliferation of LPS-stimulated B cells in a fashion dependent on the same dose escalation administered to T_H17 or T_{reg} cultures, compared with B cells activated by LPS alone, as assessed by CFSE dilution over 4 days of culture (Figure S3A). Using Fc-tagged recombinant BAFF or APRIL in combination with fluorochrome-conjugated secondary anti-Fc Ab, we also found specific binding of BAFF and APRIL ligands to splenic B cells which exceeded background binding by secondary Ab alone as anticipated (B cells; Figure S3C) but not to $CD4^+$ T cells ($CD4^+$ T cells; Figure S3C). This suggests that soluble BAFF or APRIL unlikely bound $CD4^+$

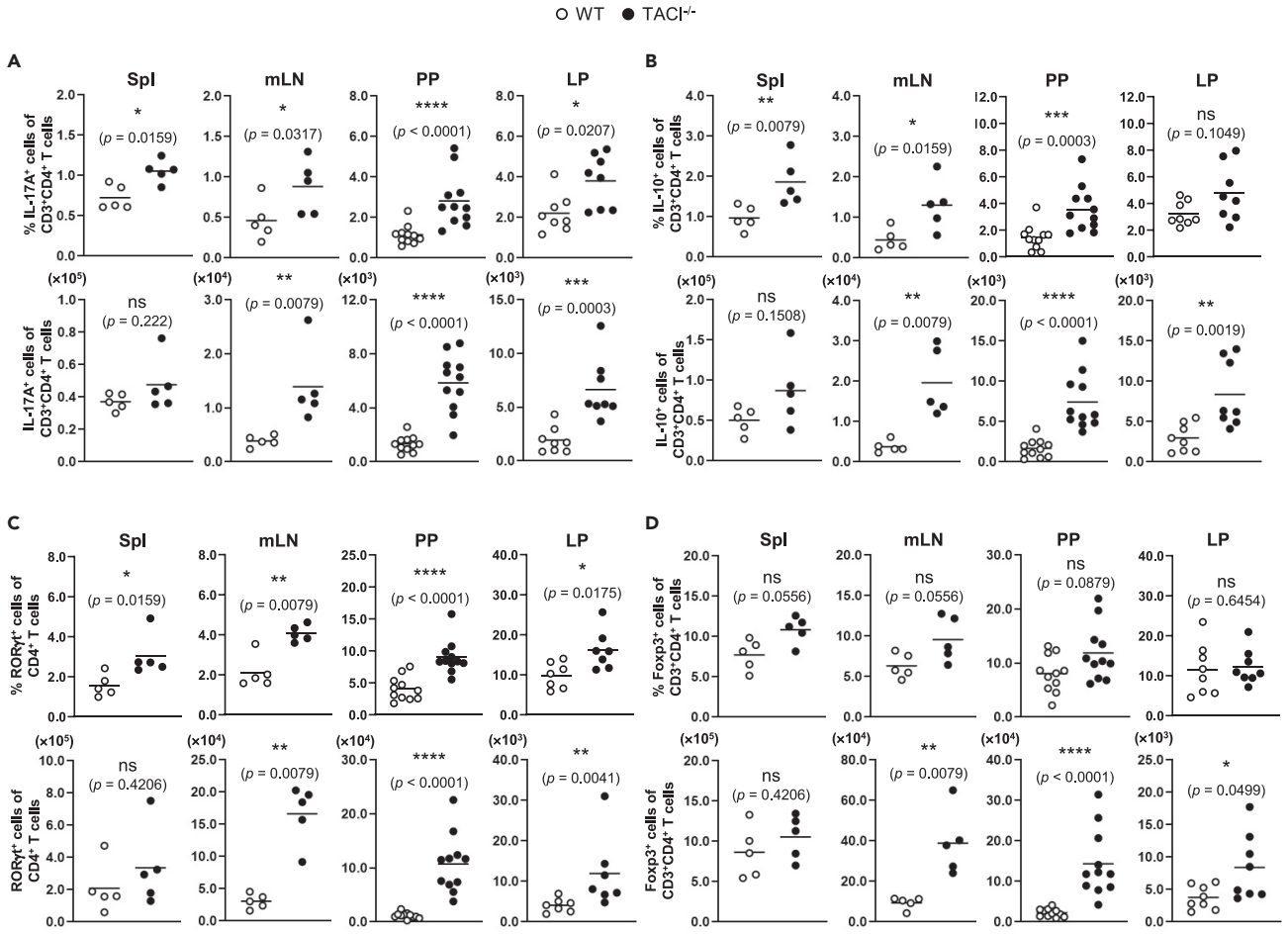

Figure 2. Accumulation of T_H17 and T_{reg} Cells in TACI$^{-/-}$ Compared with WT Mice

Cells isolated from the Spl, mLN, PP, and LP of TACI$^{-/-}$ (filled circles) or WT (open circles) mice were stimulated with PMA and ionomycin for 4 h and assessed for intracellular IL-17A (A) and IL-10 (B) expression in CD3$^+$CD4$^+$ T cells by flow cytometry. Cells from various organs of TACI$^{-/-}$ or WT mice as in (A and B) were assessed for RORγt (C) and Foxp3 (D) expression in CD3$^+$CD4$^+$ T cells. Data are based on five or more mice analyzed with each symbol representing one mouse and horizontal bars indicating the mean; Mann-Whitney U test, *, $p < 0.05$; **, $p < 0.01$; ***, $p < 0.001$; ns, not significant. Actual p values are indicated in parentheses below the asterisks or "ns."

T cells when they were added at the beginning of T_H17 and T_{reg} polarization cultures. Taken together, the preceding data allude to TACI being specifically upregulated in T_H17 cells as a negative feedback mechanism to limit their IL-17A production *in vitro* in a manner that is likely to be ligand independent.

TACI Deficiency in Mice Results in T Cell-Intrinsic Accumulation of T_H17 and T_{reg} Cells

As TACI is specifically and highly expressed in *in vitro* differentiated T_H17 and T_{reg} cells (Figure 1) and it in turn modulates T_H17 differentiation (Figure S2), we next asked what role TACI plays in T_H17 and T_{reg} development *in vivo*. To address this question, we examined the proportions of T_H17 and T_{reg} with respect to total CD3$^+$CD4$^+$ T cells in TACI$^{-/-}$ and WT mice. Using gating strategies applied to representative dot plots as depicted in Figures S4A and S4B for cells residing in lamina propria and Figure S5 for cells in each of the organs examined, we found the frequencies and numbers of IL-17A-expressing (T_H17) and IL-10-expressing (predominantly T_{reg}) CD3$^+$CD4$^+$ T cells in the spleens (Spl), mesenteric lymph nodes (mLN), Peyer's patches (PP), and lamina propria (LP) to be higher in TACI$^{-/-}$ compared with WT mice and with most differences reaching statistical significance (Figures 2A and 2B). This is consistent with higher IL-17A production by *in vitro* generated TACI$^{-/-}$ compared with WT T_H17 cells (Figure S2C). Concordantly, the frequencies and numbers of CD3$^+$CD4$^+$RORγt$^+$ T (T_H17) cells were higher in all organs examined in TACI$^{-/-}$ compared with WT mice with almost all differences reaching significance (Figure 2C). The numbers

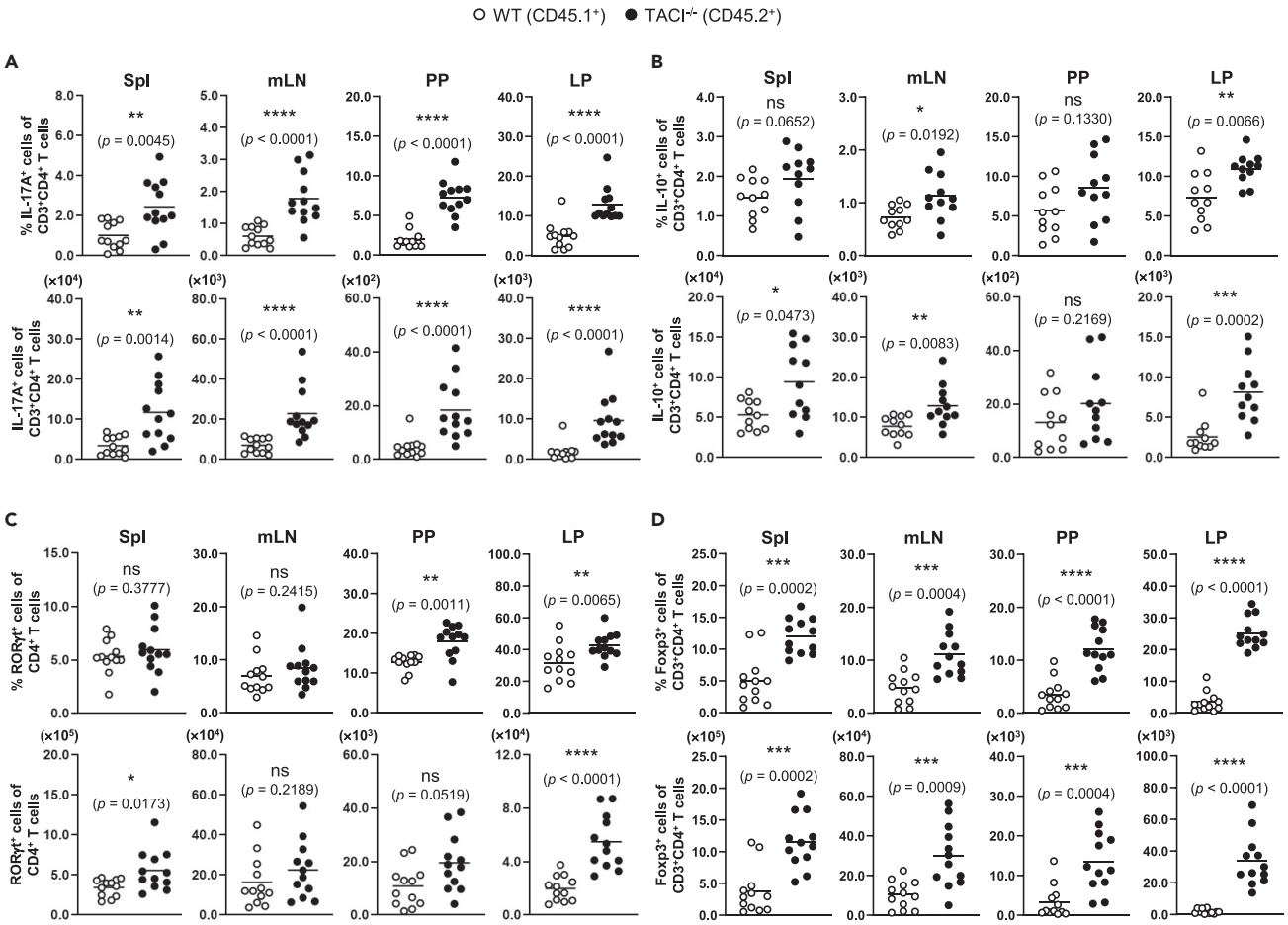

Figure 3. Expansion of T_H17 and T_{reg} Cells among $TACI^{-/-}$ versus WT $CD4^+$ T Cells in BM Chimeras

Cells isolated from the Spl, mLN, PP, and LP of BM chimeric mice were stimulated with PMA and ionomycin for 4 h and assessed for intracellular IL-17A (A) and IL-10 (B) expression in $TACI^{-/-}$ $CD45.2^+$ (filled circles) or WT $CD45.1^+$ (open circles) $CD3^+CD4^+$ T cells by flow cytometry. Cells from various organs of BM chimeric mice as in (A) and (B) were assessed for RORγt (C) and Foxp3 (D) expression in $TACI^{-/-}$ or WT $CD3^+CD4^+$ T cells. Data are based on 11 or 12 mice analyzed with each symbol representing one mouse and horizontal bars indicating the mean; Mann-Whitney U test, *, $p < 0.05$; **, $p < 0.01$; ***, $p < 0.001$; ns, not significant. Actual p values are indicated in parentheses below the asterisks or "ns."

of $CD3^+CD4^+Foxp3^+$ T (T_{reg}) cells were also significantly elevated in most organs of $TACI^{-/-}$ mice, although the proportions of $Foxp3^+$ cells in $TACI^{-/-}$ mice were not significantly different from those in WT mice (Figure 2D). In contrast, the frequencies and numbers of IFN-γ-expressing T_H1 cells (Figures S7A and S7B) and IL-4-expressing T_H2 cells (Figures S7C and S7D) in the Spl and mLN were comparable between $TACI^{-/-}$ and WT mice, consistent with similar concentrations of IFN-γ produced by $TACI^{-/-}$ and WT T_H1 and of IL-4 produced by $TACI^{-/-}$ and WT T_H2 cells differentiated *in vitro* (Figures S2A and S2B).

The accumulation of T_H17 and T_{reg} cells in $TACI^{-/-}$ mice could be T cell-intrinsic or due to T cell-extrinsic factors contributed by other immune cell types lacking TACI such as B cells, dendritic cells, or macrophages to promote the preferential differentiation of $CD4^+$ T to T_H17 and T_{reg} cells. To distinguish between these possibilities, we generated chimeric mice reconstituted with 1:1 ratio of WT ($CD45.1^+$) and $TACI^{-/-}$ ($CD45.2^+$) bone marrow (BM) cells. Similar analyses using gating strategies as depicted in Figures S4C and S4D and Figure S6 of T_H17 and T_{reg} populations in various organs of these mice revealed that the frequencies and numbers of $IL\text{-}17A^+$ (Figure 3A), $IL\text{-}10^+$ (Figure 3B), $ROR\gamma t^+$ (Figure 3C), and $Foxp3^+$ (Figure 3D) cells among $TACI^{-/-}$ $CD45.2^+CD3^+CD4^+$ T cells were significantly higher compared with those of corresponding cells among WT counterparts existing within the same microenvironment. We observed more consistent expansion of T_H17 ($IL\text{-}17A^+$) and T_{reg} ($Foxp3^+$) cells among $TACI^{-/-}$ versus WT T cells in

chimeric mice compared with T_H17 and T_{reg} cells in separate TACI$^{-/-}$ versus WT mice (Figures 3A and 3D versus Figures 2A and 2D). These data suggested that TACI$^{-/-}$ T_H17 and T_{reg} cells harbored competitive advantage over their WT counterparts in mixed chimeras, especially in gut-associated lymphoid tissues such as PP and LP, in which the elevation of TACI$^{-/-}$ and the concomitant depression of WT T_H17 and T_{reg} frequencies and numbers were most pronounced. Collectively, these results underscore the importance of TACI in attenuating T_H17 and T_{reg} but not T_H1 or T_H2 development in a T cell-intrinsic manner *in vivo*, which is correlated with the preferential expression of TACI in T_H17 and T_{reg} cells (Figure 1).

Loss of TACI Results in Greater Severity of Acute Colitis

CD3$^+$CD4$^+$ T cells, particularly T_H1 and T_H17 cells, have been shown to promote the pathogenesis of inflammatory bowel disease (IBD) and experimental colitis (Feng et al., 2011), whereas T_{reg} cells dampen IBD (Shale et al., 2013). Since TACI deficiency expanded T_H17 cells *in vivo* (Figure 2), we examined the susceptibility of TACI$^{-/-}$ and WT mice to experimental colitis. TACI$^{-/-}$ and WT mice were fed DSS *ad libitum* to induce acute colitis and monitored up to 15 days. Mice of both genotypes started losing weight 4 days post induction with TACI$^{-/-}$ mice displaying significantly more rapid weight loss compared with WT counterparts (Figure 4A). This was accompanied by greater mortality of TACI$^{-/-}$ mice, all of which succumbed to disease by day 10, whereas all WT mice survived (Figure 4B). Histological examination showed that the crypt architecture of the colons of TACI$^{-/-}$ mice was drastically perturbed with clear evidence of massive leukocyte infiltration compared with that of WT mice, which was considerably less disrupted after 6 days of DSS treatment (Figure 4D; day 6), corroborated by twice the mean histopathological score attributed to TACI$^{-/-}$ versus WT colons (Figure 4C). The presence of Ki-67$^+$ proliferating crypt cells, important for orchestrating the regeneration of intestinal epithelium following pathological damage, was also dramatically reduced in TACI$^{-/-}$ compared with WT colons (Figure 4E).

T_H17 and T_{reg} cells have been demonstrated to play reciprocal roles in promoting and suppressing the development and course of colitis (Duchmann and Zeitz, 2006; Feng et al., 2011). We examined the proportions of LP T_H17 and T_{reg} cells in TACI$^{-/-}$ and WT mice before and after 3 or 6 days of DSS administration. The frequencies of RORγt$^+$CD4$^+$ T (T_H17) cells were significantly higher in TACI$^{-/-}$ compared with WT LP at all time points examined (Figures 4F and 4G). On the other hand, the frequencies of LP Foxp3$^+$CD4$^+$ T (T_{reg}) cells were only higher in unchallenged TACI$^{-/-}$ compared with WT mice, but there was no difference in their T_{reg} frequencies during the progression of colitis (Figures 4H and 4I). Importantly, the ratios of T_H17/T_{reg} cells in TACI$^{-/-}$ mice consistently exceeded those of WT mice over 6 days of DSS challenge (Figure 4J). This imbalance in favor of T_H17 cells provides a likely explanation for the development of more severe colitis in TACI$^{-/-}$ mice.

TACI Functions in CD4$^+$ T Cells to Limit Acute and Chronic Colitis

TACI$^{-/-}$ mice are more susceptible to acute colitis (Figure 4), but it remains unclear if there exists a CD4$^+$ T cell-intrinsic role for TACI in disease susceptibility. To address this question, we generated TACI$^{-/-}$ μMT mice lacking B cells to exclude the contribution of TACI$^{-/-}$ B cells in pathogenesis. After induction of colitis in mice via DSS administration, we again observed that TACI$^{-/-}$ μMT mice lost weight more rapidly than control μMT mice (Figure 5A), albeit the difference in weight loss was not as pronounced as between B cell-sufficient TACI$^{-/-}$ and WT mice (Figure 4A). TACI$^{-/-}$ μMT colons scored higher on average versus μMT colons in histopathological features (Figure 5B) as the extent of epithelial cell loss and leukocyte infiltration was greater in colons of TACI$^{-/-}$ μMT compared with μMT mice following 6 days of DSS treatment (Figure 5C; day 6). DSS-treated TACI$^{-/-}$ μMT mice also exhibited greater mortality compared with similarly treated μMT mice (Figure 5D). These experiments eliminated the contribution of TACI in B cells and suggested that TACI acts in other leukocytes to modulate the severity of colitis.

To directly assess the function of TACI in CD4$^+$ T cells, we adoptively transferred CD4$^+$ CD62L^{hi}CD44^{lo}CD25$^-$ T_{naive} cells purified from pooled Spl and LN of TACI$^{-/-}$ or WT mice into RAG1$^{-/-}$ recipients to induce chronic colitis and monitored the recipient mice for wasting disease in terms of weight loss over a duration of 40 days. WT T_{naive} cells predictably induced progressive weight loss in RAG1$^{-/-}$ mice over 20–30 days after cell transfer. RAG1$^{-/-}$ cohorts that received TACI$^{-/-}$ T_{naive} cells, however, developed more aggressive inflammatory disease relative to RAG1$^{-/-}$ recipients of WT T_{naive} cells, as evidenced by their accelerated weight loss (Figure 5E), with divergence in percent body weight curves occurring as early as 10 days after adoptive cell transfer. TACI$^{-/-}$ T_{naive} cells inflicted substantially greater colonic damage compared with their WT counterparts in Rag1$^{-/-}$ mice as histologically scored (Figure 5F) and visualized

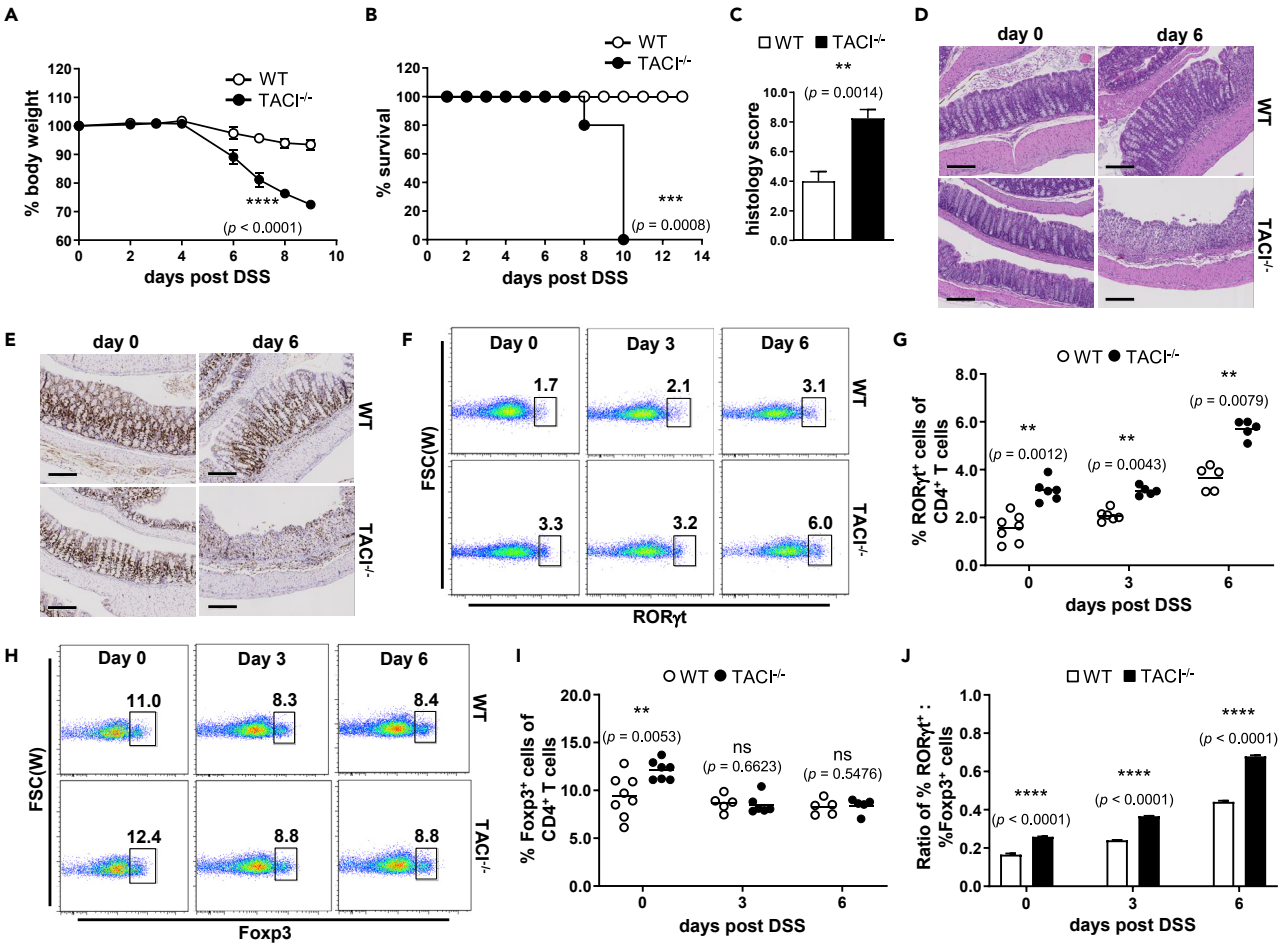

Figure 4. TACI Deficiency Led to More Severe Colitis in Mice

(A and B) The progression of wasting disease was monitored in terms of (A) change in body weights of TACI$^{-/-}$ (filled circles) and WT (open circles) mice expressed as percentage of their original weights and (B) Kaplan-Meier analysis of the survival of mice following feeding with 2% DSS in drinking water for 15 days.

(C–I) (C) Histological evaluation and scoring of DSS-induced colitis according to extent of ulceration, hyperplasia, and dysplasia, and infiltration by inflammatory cells in colons of TACI$^{-/-}$ compared with WT mice after feeding with DSS for 6 days. Degree of epithelial damage and leukocyte infiltration (D) as well as crypt cell proliferation (E) as assessed, respectively, by H&E and Ki-67 staining of colons of unchallenged (day 0) or 6-day DSS-fed mice. LP CD3$^+$CD4$^+$ T cells of unchallenged or DSS-fed mice at 3 or 6 days were assessed for RORγt (F and G) and Foxp3 (H and I) expression by flow cytometry. (J) The ratio of the frequencies of RORγt$^+$CD3$^+$CD4$^+$ to Foxp3$^+$CD3$^+$CD4$^+$ T cells in the LP of TACI$^{-/-}$ (filled bars) and WT (open bars) mice as in (G) and (I). Data in (A) and (B) are based on five male mice of each genotype; repeated-measures ANOVA, ****, $p < 0.0001$ (A); log rank (Mantel-Cox) test, ***, $p = 0.0008$ (B). Data in (C) are the mean ± SEM of histological scores of colons from eight TACI$^{-/-}$ and WT mice. Features shown in (D) and (E) are representative colon sections from one mouse each of 3 TACI$^{-/-}$ and WT mice examined. Scale bars represent 300 μm. Data in (F) to (I) are based on five or more mice analyzed with each symbol representing one mouse and horizontal bars indicating the mean; Mann-Whitney U test, **, $p < 0.01$; ns, not significant. Data in (J) are the mean ± SEM of ratios computed from five or more mice as in (G) and (I); unpaired parametric *t*-test, ****, $p < 0.0001$. Actual *p* values are indicated in parentheses below the asterisks or "ns."

by H&E staining (Figure 5I; TACI$^{-/-}$ T_{naive} versus WT T_{naive}) 30 days post cell transfer. Because T_{reg} cells, in addition to T_H17 cells, also numerically expanded in most organs of resting TACI$^{-/-}$ compared with WT mice (Figures 2D and 4I), we asked if TACI$^{-/-}$ T_{reg} cells were functionally competent to suppress colitis. To address this, WT T_{naive} cells were transferred alone or concurrently with TACI$^{-/-}$ or WT CD4$^+$CD62L^{hi}CD44^{lo}CD25$^+$ T_{reg} cells into RAG1$^{-/-}$ mice. As expected, mice receiving WT T_{naive} cells alone progressively shed weight, which was completely prevented by the co-transfer of WT T_{reg} cells (Figure 5G; WT T_{naive} + WT T_{reg} versus WT T_{naive}), a finding corroborated by the lower mean histological score (Figure 5H) and degree of pathology (Figure 5I) of colons from Rag1$^{-/-}$ mice that received WT T_{naive} together with WT T_{reg} versus those that received WT T_{naive} cells alone. Importantly, co-transferred TACI$^{-/-}$ T_{reg} suppressed

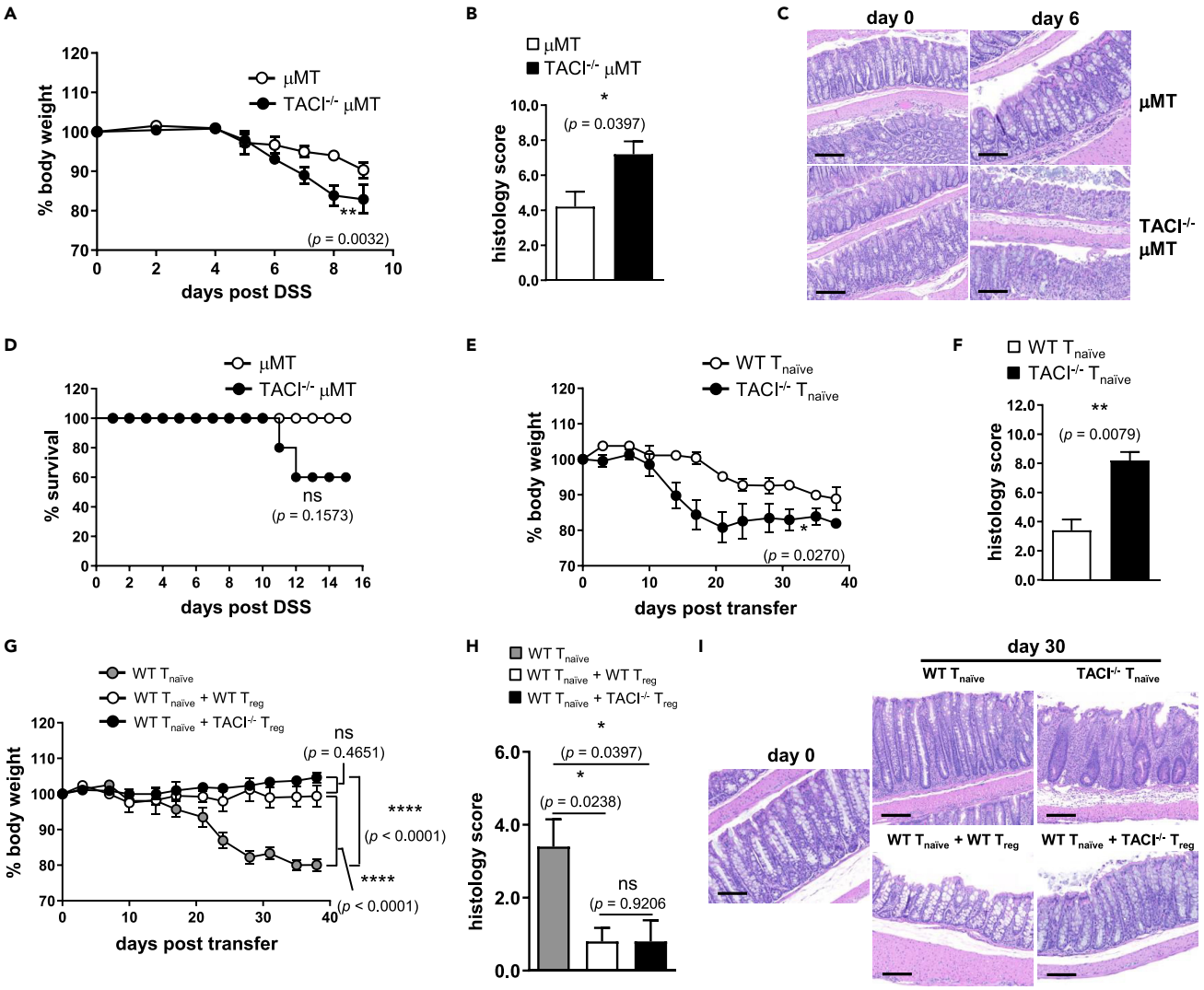

Figure 5. CD4$^+$ T Cell-Intrinsic Role of TACI in Colitis

Change in body weights as percentage of original weights (A) and Kaplan-Meier survival analysis (D) of TACI$^{-/-}$ μMT (filled circles) compared with μMT (open circles) control mice after feeding with DSS in drinking water for 15 days. Histological scoring (B) and H&E assessment (C) of colitis in colons of unchallenged (day 0) or 6-day DSS-fed TACI$^{-/-}$ μMT and μMT mice. Percentage change in body weight curves of RAG1$^{-/-}$ mice that received TACI$^{-/-}$ (filled circles) or WT (open circles) CD4$^+$CD62L^{hi}CD44^{lo}CD25$^-$ T_{naive} cells (E), WT T_{naive} cells only (gray circles) or concurrently with TACI$^{-/-}$ (black circles) or WT (open circles) CD4$^+$CD62L^{hi}CD44^{lo}CD25$^+$ T_{reg} cells (G). Histological scoring (F and H) and H&E assessment (I) of colitis in colons of RAG1$^{-/-}$ mice at day 0 (before cell transfer) or 30 days after receiving T_{naive} or T_{naive} in combination with T_{reg} cells from mice of genotypes described in (E) and (G). Scale bars in (C) and (I) represent 200 μm. Data in (A) and (D) are based on five female mice of each genotype; repeated-measures ANOVA, **, $p = 0.0032$ (A); log rank (Mantel-Cox) test, ns, $p = 0.1573$ (D). Data in (B) are the mean ± SEM of histological scores of colons from five TACI$^{-/-}$ μMT and μMT mice. Features shown in (C) are representative colon sections from one mouse each of three TACI$^{-/-}$ μMT and μMT mice examined. Data in (E) and (G) are based on five female RAG1$^{-/-}$ recipient mice in each cohort receiving TACI$^{-/-}$ or WT T_{naive} cells; repeated-measures ANOVA, **, $p = 0.0270$ (E) or WT T_{naive} in combination with TACI$^{-/-}$ or WT T_{reg} cells; ****, $p < 0.0001$; ns, $p = 0.4651$ (G). Data in (F) and (H) are the mean ± SEM of histological scores of colons from five RAG1$^{-/-}$ mice. Features shown in (I) are representative colon sections from one mouse of five RAG1$^{-/-}$ mice in each cohort examined. ns, not significant. Actual p values are indicated in parentheses below the asterisks or "ns."

disease evoked by WT T_{naive} cells as efficaciously as WT T_{reg} cells (Figure 5G; WT T_{naive} + TACI$^{-/-}$ T_{reg} versus WT T_{naive} + WT T_{reg}), which was confirmed by histological scoring and examination (Figures 5H and 5I; WT T_{naive} + TACI$^{-/-}$ T_{reg} versus WT T_{naive} + WT T_{reg}), suggesting no defect in TACI$^{-/-}$ T_{reg} function. Taken together, the above data argue for a CD4$^+$ T cell-autonomous requirement of TACI in limiting T_H17-mediated colitis. These conclusions are consistent with a CD4$^+$ T cell-intrinsic role for TACI in constraining T_H17 differentiation *in vivo* (Figure 3).

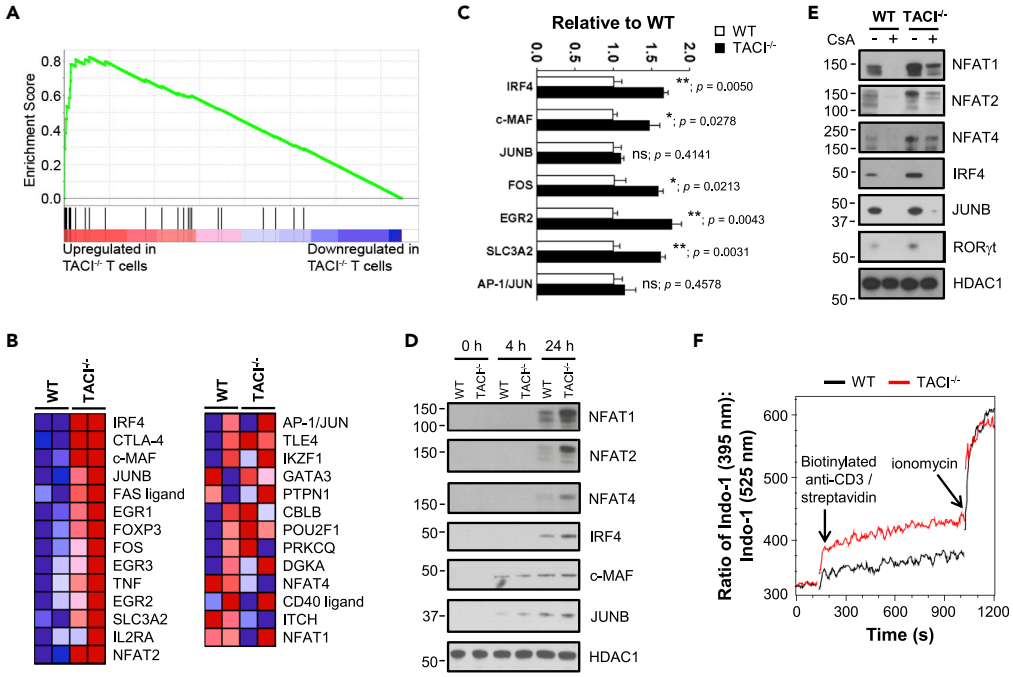

Figure 6. Augmented Expression of NFAT-Dependent Transcriptional Pathway Promoting T_H17 Development in TACI$^{-/-}$ T_{naive} Cells

(A) GSEA-based enrichment plot of the calcineurin-regulated NFAT-dependent transcriptional pathway (normalized enrichment score = 2.42; FDR *q*-value < 0.001) based on microarray analysis of T_{naive} cells FACS-sorted as in Figures 5C and 5D from pooled Spl and LN of TACI$^{-/-}$ and WT mice (n = 2 each). Vertical black lines indicate genes for which expression was detected by microarray as listed in (B).

(B) Expression heatmap of genes involved in regulation of the pathway as described in (A). Columns represent WT or TACI$^{-/-}$ T_{naive} cells derived from two mice of each genotype. Red and blue denote high and low transcript expression levels, respectively.

(C) Transcript levels of T_H17-associated genes in WT (open bars) and TACI$^{-/-}$ (filled bars) T_{naive} cells as assessed by quantitative real-time PCR.

(D and E) Expression of T_H17-associated proteins in the nuclei of WT and TACI$^{-/-}$ T_{naive} cells at 0, 4, and 24 h stimulation with anti-CD3 and anti-CD28 Abs (D) or 24 h culture in T_H17-polarizing conditions in the presence or absence of CsA as assessed by western blotting (E). Levels of HDAC1 serve as loading control.

(F) Real-time intracellular calcium flux in WT or TACI$^{-/-}$ CD4$^+$ T cells stimulated with biotinylated anti-CD3 Ab and streptavidin as assessed by flow cytometry.

Data in (C) are the mean ± SEM of three technical replicates and representative of two independent experiments; unpaired parametric *t*-test; *, $p < 0.05$; **, $p < 0.01$; ns, not significant. Actual *p* values are indicated adjacent to the asterisks or "ns." Data in (D)–(F) are representative of two independent experiments showing similar results.

CD4$^+$ T Cells Lacking TACI Exhibited Enhanced Activation of T_H17-Promoting Transcription Factors

To understand the mechanisms underlying increased frequency of T_H17 cells associated with aggravated colitis in TACI$^{-/-}$ mice, we performed microarray-based transcriptome analysis to identify genes that were differentially expressed (DEGs) in TACI$^{-/-}$ versus WT T_{naive} cells that were FACS-sorted from pooled Spl and LN of mice. We identified 97 genes that were significantly upregulated and 66 genes that were significantly downregulated in TACI$^{-/-}$ compared with WT T_{naive} cells (absolute fold change >1.5, $p < 0.05$). Gene Set Enrichment Analysis (GSEA, http://software.broadinstitute.org/gsea/index.jsp; Subramanian et al., 2005) comprising gene sets from Pathway Interaction Database, BioCarta, KEGG, Reactome, and Gene Ontology revealed that genes of the calcineurin-regulated NFAT-dependent transcriptional pathway were the most significantly upregulated in TACI$^{-/-}$ versus WT T_{naive} cells compared with other signaling pathways (Figure 6A; normalized enrichment score = 2.42, FDR *q*-value < 0.001). Indeed, expression of genes involved in the NFAT pathway were found to be significantly changed (restricted to those with fold change >1.5; unpaired *t*-test, $p < 0.05$; Figure 6B). Notably, the list of genes, all of which have been

shown to regulate T_H17 differentiation, included NFAT1 and 2 (Dietz et al., 2015; Reppert et al., 2015), IRF4 (Brüstle et al., 2007; Gaffen et al., 2014; Huber et al., 2008), c-MAF (Bauquet et al., 2009; Gabryšová et al., 2018), solute carrier 3A2 (SLC3A2; Kurihara et al., 2015), Fos proto-oncogene (FOS) and JUNB (Carr et al., 2017; Hasan et al., 2017; Moon et al., 2017; Schraml et al., 2009), and early growth response 2 (EGR2; Du et al., 2014). Increased expression of some of these T_H17-associated genes in TACI$^{-/-}$ compared with WT T_{naive} cells was subsequently verified by quantitative real-time PCR (Figure 6C), although the increase in levels of JUNB and AP-1 transcripts did not reach statistical significance. Notably, when WT and TACI$^{-/-}$ T_{naive} cells were activated with anti-CD3 and anti-CD28 Abs for 4 and 24 h, we observed increased localization of NFAT1, NFAT2, NFAT4, IRF4, c-MAF, and JUNB proteins in the nuclei of TACI$^{-/-}$ compared with WT T_{naive} cells, suggesting increased activation of the mutant T cells, particularly after 24 h of stimulation (Figure 6D). Similarly, exaggerated levels of nuclear NFATs, IRF4, JUNB, and RORγt were also observed in TACI$^{-/-}$ T_{naive} cells activated under T_H17-polarizing conditions for 24 h (Figures 6E and S8), indicating hyper-activation of these transcription factors in TACI$^{-/-}$ cells undergoing T_H17 differentiation. Treatment for 24 h with cyclosporin A (CsA), a well-known calcineurin inhibitor that dampens NFAT activation, abolished the nuclear translocation of IRF4, JUNB, and RORγt proteins in both WT and TACI$^{-/-}$ cells (Figures 6E and S8). Nuclear expression of NFAT 1, 2, and 4, however, was extinguished in WT but only reduced in TACI$^{-/-}$ cells at the CsA concentration applied, suggesting that TACI$^{-/-}$ T_{naive} cells harbored higher levels of activated NFAT than WT counterparts. Since NFATs have been implicated in transcriptional activation of IRF4 (Biswas et al., 2010) and RORγt (Zhou and Littman, 2009), our data are consistent with a model in which loss of TACI promotes the activation of IRF4 and RORγt via increased NFAT induction.

NFAT activation is highly dependent on calcium influx (Gabriel et al., 2016; Macian, 2005). Hence, we next measured intracellular calcium flux in WT and TACI$^{-/-}$ CD4$^+$ T cells. Upon stimulation with biotinylated anti-CD3 Ab and streptavidin, TACI$^{-/-}$ cells accumulated calcium to a greater degree than WT cells as visualized by increased levels of Indo-1-bound intracellular calcium (Figure 6F), in agreement with heightened resistance of TACI$^{-/-}$ cells to CsA-mediated inhibition of NFAT activation. This greater amplitude of intracellular calcium was sustained till the addition of ionomycin, which triggered the same expected calcium spike in both WT and TACI$^{-/-}$ cells (Figure 6F). Moreover, TCRβ expression in WT and TACI$^{-/-}$ T_{naive} cells, whether left unstimulated or stimulated with anti-CD3 and anti-CD28 Abs for 24 h, was comparable (Figure S9), clarifying that the higher calcium influx in TACI$^{-/-}$ cells was not due to increased TCRβ expression.

DISCUSSION

Extensive studies have delineated enigmatic but yet important functions for TACI in B cells, which highly express the receptor at later stages of their differentiation. These include inhibition of B cell proliferation and GC B cell formation (Ou et al., 2012; Yan et al., 2001) but promotion of plasma cell survival and Ig class switch recombination (Figgett et al., 2015; He et al., 2010; Ou et al., 2012; Salzer et al., 2007; Seshasayee et al., 2003). TACI is weakly expressed in dendritic cells (Wu et al., 2000) and macrophages (Allman et al., 2015), whereas its expression and function in T cells remain controversial (Mackay and Leung, 2006; Ng et al., 2004; Seyler et al., 2005; Von Bülow and Bram, 1997; Wu et al., 2000).

Although TACI was shown to be upregulated in mouse T cells activated with PMA and ionomycin (Von Bülow and Bram, 1997), it is unclear whether TCR- and/or cytokine-mediated signals induce TACI expression and whether TACI plays a physiological role in T cell function. We showed that activation of T_{naive} cells with anti-CD3 and anti-CD28 Abs alone was insufficient to induce TACI expression in CD4$^+$ T_{naive} cells. However, TACI expression could be induced by administering the anti-inflammatory T_H17 and T_{reg}-promoting cytokine TGF-β to activated T cells and this effect was enhanced by IL-6 but not IL-2. In contrast, cytokines directing T_H1 and T_H2 commitment failed to induce TACI expression in T cells. Although extensive studies demonstrated that BAFF can co-stimulate proliferation of TCR-activated T cells, only a very small subset of 2%–3% of murine splenic T cells expresses BAFF-R at steady state and this expression increased 2-fold upon activation (Huard et al, 2001, 2004; Ng et al., 2004; Scapini et al., 2010; Ye et al., 2004). Unlike TACI expression, which was substantially increased, BAFF-R expression was slightly increased, whereas BMCA was not expressed in T_H17 and T_{reg} cells. Further studies are needed to more carefully assess if expression of TACI, BAFF-R, and BCMA in CD4$^+$ T cells under various polarizing conditions changes at culture time points not examined in the current study or when strong mitogens such as PMA are utilized to activate T cells. Nevertheless, our current data suggest BAFF-R and BCMA, compared with TACI, may not play a major role in regulating T_H17 and T_{reg} differentiation.

Given the selective expression of TACI in T_H17 and T_{reg} cells, we investigated a possible role of TACI in T_H17 and T_{reg} development. TACI$^{-/-}$ T_H17 cells differentiated *in vitro* produced significantly higher concentration of IL-17A compared with their WT counterparts. Consistent with this, the homeostatic proportions of T_H17 and T_{reg} cells in Spl, mLN, PP, and LP were consistently elevated in TACI$^{-/-}$ compared with WT mice and among TACI$^{-/-}$ versus WT CD4$^+$ T cells in BM chimeras, with the most pronounced increases observed in the PP and LP. This may be due to the much higher concentration of TGF-β in the gut (including PP and LP) compared with Spl and mLN (Neurath, 2014). These data suggest that T_H17 and T_{reg} accumulation in TACI$^{-/-}$ mice is T cell-intrinsic and that TACI in WT CD4$^+$ T cells constrains T_H17 and T_{reg} development. To determine if the latter requires binding of BAFF or APRIL ligand to TACI, we added BAFF or APRIL to CD4$^+$ T cells at the beginning of T_H17 or T_{reg} polarization and found neither cytokine reduced T_H17 or T_{reg} frequencies at the end of culture. This was likely because neither BAFF nor APRIL bound CD4$^+$ T cells when added at the start of T_H17 and T_{reg} culture. It is plausible that low levels of TACI expressed in initially polarizing T_H17 and T_{reg} cells are saturated by endogenous BAFF and APRIL and thus unable to bind exogenous cytokines. Alternatively, TACI expressed in T_H17 and T_{reg} cells may only bind membrane-bound but not soluble BAFF or APRIL. It also remains possible that BAFF or APRIL binds T_H17 and T_{reg} cells to modulate their cytokine expression and survival beyond the differentiation period of 3 days. These hypotheses warrant future investigation to determine whether the functions of TACI in CD4$^+$ T cells depend on interaction with its ligands BAFF and/or APRIL.

Since T_H17 cells have been implicated in the pathogenesis of IBD (Feng et al., 2011; Shale et al., 2013), we chemically induced colitis in mice, which revealed that TACI deficiency led to worsened wasting disease, which was accompanied by increased mortality. There was more severe epithelial tissue destruction attributable to markedly reduced presence of proliferating crypt cells that facilitate tissue repair. Because of the prominent function of TACI in B cells and its role in promoting IgA class switching, we eliminated the contribution of B cells by generating TACI$^{-/-}$ mice devoid of B cells (TACI$^{-/-}$ μMT mice) and found that TACI deficiency in the absence of B cells again led to manifestation of more severe colitis. Furthermore, adoptive transfer of TACI$^{-/-}$ T_{naive} cells into RAG1$^{-/-}$ mice evoked more severe disease, which, together with findings from TACI$^{-/-}$ μMT mice, argued for a CD4$^+$ T cell-autonomous requirement for TACI in alleviating colitis. However, we cannot rule out the possibility that TACI may nonetheless function in B cells to modulate colitis since disease severity in TACI$^{-/-}$ μMT versus control μMT mice was less than B cell-sufficient TACI$^{-/-}$ versus WT mice. Moreover, dendritic cells (Wu et al., 2000) and macrophages (Allman et al., 2015), which weakly express TACI, could also regulate colitis. The relative contributions of TACI function in T cells, B cells, dendritic cells, and macrophages to colitis await the generation of mice with the TACI gene ablated conditionally in these cell types.

To understand why TACI$^{-/-}$ CD4$^+$ T cells have propensity to adopt T_H17 phenotype, we conducted microarray analysis of TACI$^{-/-}$ versus WT T_{naive} cells, which revealed that the former over-expressed a constellation of T_H17-associated genes constituting the NFAT-dependent transcriptional pathway, including transcription factors NFAT, IRF4, c-MAF, and JUNB known to promote T_H17 differentiation and the production of signature T_H17 cytokines (Hermann-Kleiter and Baier, 2010). T_{naive} rather than total CD4$^+$ T cells were employed to avoid analysis of DEGs being confounded by increased proportions of activated T cells in resting TACI$^{-/-}$ compared with WT mice. TACI$^{-/-}$ CD4$^+$ T cells fluxed aberrantly higher levels of calcium that promote enhanced dephosphorylation of cytoplasmic NFATs by calcineurin and accelerated nuclear import of NFATs (Macian, 2005), thereby increasing NFAT, IRF4, and RORγt activation. These data suggest that the suppression of the calcineurin-NFAT signaling axis by TACI in CD4$^+$ T cells inhibits T_H17 development, similar to what was earlier observed in B cells (Ou et al., 2012). Elucidation of how TACI specifically restricts signaling by components of the NFAT pathway in CD4$^+$ T cells will be the subject of future investigation. This is crucial to devising interventions that cripple T_H17-mediated pathology in IBD without excessively compromising TACI-mediated functions in other immune cell types that are important to preserve intestinal homeostasis, e.g., production of gut IgA by B and plasma cells (Cerutti and Rescigno, 2008).

TACI has been shown to play opposing, context-dependent roles in the pathogenesis of autoimmune disease that include promoting inflammation and joint destruction in collagen-induced arthritis (Wang et al., 2001), autoantibody production in systemic lupus erythematosus (Figgett et al., 2015), and Ig transcription in GC+ synovitis while limiting IFN-γ production in aggregate and diffuse synovitis (Seyler et al., 2005). Our current data support a working model in which TACI is induced selectively in CD4$^+$ T cells

differentiating into the T_H17 lineage and in turn constrains their activation and pathogenicity by restricting their levels of intracellular calcium flux to limit T_H17 responses. Besides extending the diverse roles TACI plays in various immune cell types to $CD4^+$ T cells, our findings advance the understanding of the context-specific mechanisms governing TACI function that will inform the development of new therapeutics to target TACI for the amelioration of autoimmune diseases, infection, and cancer.

LIMITATIONS OF THE STUDY

We initially observed accumulation of T_H17 and T_{reg} cells in $TACI^{-/-}$ mice that could be attributed to T cell-intrinsic effects or extrinsic factors produced by other immune cell types lacking TACI. We then generated chimeric mice reconstituted with equal numbers of congenically distinguished WT and $TACI^{-/-}$ bone marrow (BM) cells to clarify that TACI functions intrinsically in $CD4^+$ T cells to constrain T_H17 and T_{reg} differentiation. Limitations of the chimeric system include variability in BM reconstitution of irradiated mice as well as perturbations of the gut microbiome induced by antibiotics administered to mice shortly following irradiation to minimize opportunistic infections. To overcome these, future studies could consider engineering *Tnfrsf13b* (encoding TACI) floxed ($Tnfrsf13b^{f/f}$) mice and crossing them to $Cd4^{cre}$ mice to generate mice harboring T cell-specific deletion of TACI. These $Tnfrsf13b^{f/f}Cd4^{Cre}$ mice will provide an independent model to substantiate findings in the current study using $TACI^{-/-}$ and BM chimeric mice. Furthermore, crossing $Tnfrsf13b^{f/f}$ mice to commercially available $Il17^{cre}$ or $Foxp3^{cre}$ mice will enable more specific dissection of the roles of TACI in T_H17 and T_{reg} populations. Whether and how TACI deficiency affects the gut microbiome and in turn contributes to colitis pathogenesis remains to be examined.

Resource Availability

Materials Availability

This study did not generate new unique reagents.

Data and Code Availability

Microarray data were deposited in NCBI with accession number GSE152077 (https://www.ncbi.nlm.nih.gov/geo/query/acc.cgi?acc=GSE152077).

METHODS

All methods can be found in the accompanying Transparent Methods supplemental file.

SUPPLEMENTAL INFORMATION

Supplemental Information can be found online at https://doi.org/10.1016/j.isci.2020.101707.

ACKNOWLEDGMENTS

We thank staff of the Biological Resource Centre (BRC) for care and maintenance of mice and members of the laboratory for insightful discussions. The Advanced Molecular Pathology Laboratory (AMPL) of the Institute of Molecular and Cell Biology assisted in the preparation and histological staining of colon samples. This research was supported by Bioprocessing Technology Institute, Agency for Science, Technology and Research, Singapore (A*STAR).

AUTHOR CONTRIBUTIONS

A.H.-M.T., G.H.W.T., P.-Y.T., X.O., and K.-P.L. conceived and designed the study. G.H.W.T., B.Z., P.-Y.T., X.O., S.-W.N., A.X.F.W., S.J.X.T., A.S., and S.S.-Y.K. performed experiments and generated data. A.H.-M.T., B.Z., G.H.W.T., P.-Y.T., X.O., S.-W.N., A.P.L., S.X., and K.-P.L. analyzed data. A.H.-M.T. and K.-P.L. supervised the study, interpreted data, and wrote the manuscript. All authors reviewed and approved the manuscript.

DECLARATION OF INTERESTS

The authors declare no competing interests.

Received: May 15, 2019
Revised: May 20, 2020
Accepted: October 7, 2020
Published: November 20, 2020

REFERENCES

Allman, W.R., Dey, R., Liu, L., Siddiqui, S., Coleman, A.S., Bhattacharya, P., Yano, M., Uslu, K., Takeda, K., Nakhasi, H.L., and Akkoyunlu, M. (2015). TACI deficiency leads to alternatively activated macrophage phenotype and susceptibility to Leishmania infection. Proc. Natl. Acad. Sci. U S A *112*, E4094–E4103.

Bauquet, A.T., Jin, H., Paterson, A.M., Mitsdoerffer, M., Ho, I.C., Sharpe, A.H., and Kuchroo, V.K. (2009). The costimulatory molecule ICOS regulates the expression of c-Maf and IL-21 in the development of follicular T helper cells and TH -17 cells. Nat. Immunol. *10*, 167–175.

Biswas, P.S., Bhagat, G., and Pernis, A.B. (2010). IRF4 and its regulators: evolving insights into the pathogenesis of inflammatory arthritis? Immunol. Rev. *233*, 79–96.

Bossen, C., Cachero, T.G., Tardivel, A., Ingold, K., Willen, L., Dobles, M., Scott, M.L., Maquelin, A., Belnoue, E., Siegrist, C.A., et al. (2008). TACI, unlike BAFF-R, is solely activated by oligomeric BAFF and APRIL to support survival of activated B cells and plasmablasts. Blood *111*, 1004–1012.

Brüstle, A., Heink, S., Huber, M., Rosenplänter, C., Stadelmann, C., Yu, P., Arpaia, E., Mak, T.W., Kamradt, T., and Lohoff, M. (2007). The development of inflammatory TH-17 cells requires interferon-regulatory factor 4. Nat. Immunol. *8*, 958–966.

Carr, T.M., Wheaton, J.D., Houtz, G.M., and Ciofani, M. (2017). JunB promotes Th17 cell identity and restrains alternative CD4+ T-cell programs during inflammation. Nat. Commun. *8*, 301.

Cerutti, A., and Rescigno, M. (2008). The biology of intestinal immunoglobulin A responses. Immunity *28*, 740–750.

Dietz, L., Frommer, F., Vogel, A.L., Vaeth, M., Serfling, E., Waisman, A., Buttmann, M., and Berberich-Siebelt, F. (2015). NFAT1 deficit and NFAT2 deficit attenuate EAE via different mechanisms. Eur. J. Immunol. *45*, 1377–1389.

Du, N., Kwon, H., Li, P., West, E.E., Oh, J., Liao, W., Yu, Z., Ren, M., and Leonard, W.J. (2014). EGR2 is critical for peripheral naíve T-cell differentiation and the T-cell response to influenza. Proc. Natl. Acad. Sci. U S A *111*, 16484–16489.

Duchmann, R., and Zeitz, M. (2006). T regulatory cell suppression of colitis: the role of TGF-β. Gut *55*, 604–606.

Feng, T., Qin, H., Wang, L., Benveniste, E.N., Elson, C.O., and Cong, Y. (2011). Th17 cells induce colitis and promote Th1 cell responses through IL-17 induction of innate IL-12 and IL-23 production. J. Immunol. *186*, 6313–6318.

Figgett, W.A., Deliyanti, D., Fairfax, K.A., Quah, P.S., Wilkinson-Berka, J.L., and Mackay, F. (2015). Deleting the BAFF receptor TACI protects against systemic lupus erythematosus without extensive reduction of B cell numbers. J. Autoimmun. *61*, 9–16.

Gabriel, C.H., Gross, F., Karl, M., Stephanowitz, H., Hennig, A.F., Weber, M., Gryzik, S., Bachmann, I., Hecklau, K., Wienands, J., et al. (2016). Identification of novel nuclear factor of activated T cell (NFAT)-associated proteins in T cells. J. Biol. Chem. *291*, 24172–24187.

Gabryšová, L., Alvarez-Martinez, M., Luisier, R., Cox, L.S., Sodenkamp, J., Hosking, C., Pérez-Mazliah, D., Whicher, C., Kannan, Y., Potempa, K., et al. (2018). C-Maf controls immune responses by regulating disease-specific gene networks and repressing IL-2 in CD4+ T cells article. Nat. Immunol. *19*, 497–507.

Gaffen, S.L., Jain, R., Garg, A.V., and Cua, D.J. (2014). The IL-23-IL-17 immune axis: from mechanisms to therapeutic testing. Nat. Rev. Immunol. *14*, 585–600.

Hasan, Z., Koizumi, S.I., Sasaki, D., Yamada, H., Arakaki, N., Fujihara, Y., Okitsu, S., Shirahata, H., and Ishikawa, H. (2017). JunB is essential for IL-23-dependent pathogenicity of Th17 cells. Nat. Commun. *8*, 15628.

He, B., Santamaria, R., Xu, W., Cols, M., Chen, K., Puga, I., Shan, M., Xiong, H., Bussel, J.B., Chiu, A., et al. (2010). The transmembrane activator TACI triggers immunoglobulin class switching by activating B cells through the adaptor MyD88. Nat. Immunol. *11*, 836–845.

Hermann-Kleiter, N., and Baier, G. (2010). NFAT pulls the strings during CD4+ T helper cell effector functions. Blood *115*, 2989–2997.

Huard, B., Arlettaz, L., Ambrose, C., Kindler, V., Mauri, D., Roosnek, E., Tschopp, J., Schneider, P., and French, L.E. (2004). BAFF production by antigen-presenting cells provides T cell co-stimulation. Int. Immunol. *16*, 467–475.

Huard, B., Schneider, P., Mauri, D., Tschopp, J., and French, L.E. (2001). T cell costimulation by the TNF ligand BAFF. J. Immunol. *167*, 6225–6231.

Huber, M., Brüstle, A., Reinhard, K., Guralnik, A., Walter, G., Mahiny, A., Von Löw, E., and Lohoff, M. (2008). IRF4 is essential for IL-21-mediated induction, amplification, and stabilization of the Th17 phenotype. Proc. Natl. Acad. Sci. U S A *105*, 20846–20851.

Kurihara, T., Arimochi, H., Bhuyan, Z.A., Ishifune, C., Tsumura, H., Ito, M., Ito, Y., Kitamura, A., Maekawa, Y., and Yasutomo, K. (2015). CD98 heavy chain is a potent positive regulator of CD4+ T cell proliferation and interferon-γ production in vivo. PLoS One *10*, e0139692.

Macian, F. (2005). NFAT proteins: key regulators of T-cell development and function. Nat. Rev. Immunol. *5*, 472–484.

Mackay, F., and Leung, H. (2006). The role of the BAFF/APRIL system on T cell function. Semin. Immunol. *18*, 284–289.

Mackay, F., and Schneider, P. (2008). TACI, an enigmatic BAFF/APRIL receptor, with new unappreciated biochemical and biological properties. Cytokine Growth Factor Rev. *19*, 263–276.

Moon, Y.M., Lee, S.Y., Kwok, S.K., Lee, S.H., Kim, D., Kim, W.K., Her, Y.M., Son, H.J., Kim, E.K., Ryu, J.G., et al. (2017). The fos-related antigen 1-JUNB/activator protein 1 transcription complex, a downstream target of signal transducer and activator of transcription 3, induces T helper 17 differentiation and promotes experimental autoimmune arthritis. Front. Immunol. *8*, 1793.

Neurath, M.F. (2014). Cytokines in inflammatory bowel disease. Nat. Rev. Immunol. *14*, 329–342.

Ng, L.G., Sutherland, A.P.R., Newton, R., Qian, F., Cachero, T.G., Scott, M.L., Thompson, J.S., Wheway, J., Chtanova, T., Groom, J., et al. (2004). B cell-activating factor belonging to the TNF family (BAFF)-R is the principal BAFF receptor facilitating BAFF costimulation of circulating T and B cells. J. Immunol. *173*, 807–817.

Ou, X., Xu, S., and Lam, K.P. (2012). Deficiency in TNFRSF13B (TACI) expands T-follicular helper and germinal center B cells via increased ICOS-ligand expression but impairs plasma cell survival. Proc. Natl. Acad. Sci. U S A *109*, 15401–15406.

Reppert, S., Zinser, E., Holzinger, C., Sandrock, L., Koch, S., and Finotto, S. (2015). NFATc1 deficiency in T cells protects mice from experimental autoimmune encephalomyelitis. Eur. J. Immunol. *45*, 1426–1440.

Rickert, R.C., Jellusova, J., and Miletic, A.V. (2011). Signaling by the tumor necrosis factor receptor superfamily in B-cell biology and disease. Immunol. Rev. *244*, 115–133.

Salzer, U., Jennings, S., and Grimbacher, B. (2007). To switch or not to switch - the opposing roles of TACI in terminal B cell differentiation. Eur. J. Immunol. *37*, 17–20.

Scapini, P., Hu, Y., Chu, C.L., Migone, T.S., DeFranco, A.L., Cassatella, M.A., and Lowell, C.A. (2010). Myeloid cells, BAFF, and IFN-γ establish an inflammatory loop that exacerbates autoimmunity in Lyn-deficient mice. J. Exp. Med. *207*, 1757–1773.

Schraml, B.U., Hildner, K., Ise, W., Lee, W.L., Smith, W.A.E., Solomon, B., Sahota, G., Sim, J., Mukasa, R., Cemerski, S., et al. (2009). The AP-1 transcription factor Batf controls T H 17 differentiation. Nature *460*, 405–409.

Seshasayee, D., Valdez, P., Yan, M., Dixit, V.M., Tumas, D., and Grewal, I.S. (2003). Loss of TACI causes fatal lymphoproliferation and

autoimmunity, establishing TACI as an inhibitory BLyS receptor. Immunity *18*, 279–288.

Seyler, T.M., Park, Y.W., Takemura, S., Bram, R.J., Kurtin, P.J., Goronzy, J.J., and Weyand, C.M. (2005). BLyS and APRIL in rheumatoid arthritis. J. Clin. Invest. *115*, 3083–3092.

Shale, M., Schiering, C., and Powrie, F. (2013). CD4+ T-cell subsets in intestinal inflammation. Immunol. Rev. *252*, 164–182.

Subramanian, A., Tamayo, P., Mootha, V.K., Mukherjee, S., Ebert, B.L., Gillette, M.A., Paulovich, A., Pomeroy, S.L., Golub, T.R., Lander, E.S., and Mesirov, J.P. (2005). Gene set enrichment analysis: a knowledge-based approach for interpreting genome-wide expression profiles. Proc. Natl. Acad. Sci. U. S. A *102*, 15545–15550.

Von Bülow, G.U., and Bram, R.J. (1997). NF-AT activation induced by a CAML-interacting member of the tumor necrosis factor receptor superfamily. Science *278*, 138–141.

Wang, H., Marsters, S.A., Baker, T., Chan, B., Lee, W.P., Fu, L., Tumas, D., Yan, M., Dixit, V.M., Ashkenazi, A., and Grewal, I.S. (2001). TACI-ligand interactions are required for T cell activation and collagen-induced arthritis in mice. Nat. Immunol. *2*, 632–637.

Wu, Y., Bressette, D., Carrell, J.A., Kaufman, T., Feng, P., Taylor, K., Gan, Y., Cho, Y.H., Garcia, A.D., Gollatz, E., et al. (2000). Tumor necrosis factor (TNF) receptor superfamily member TACI is a high affinity receptor for TNF family members APRIL and BLyS. J. Biol. Chem. *275*, 35478–35485.

Yan, M., Wang, H., Chan, B., Roose-Girma, M., Erickson, S., Baker, T., Tumas, D., Grewal, I.S., and Dixit, V.M. (2001). Activation and accumulation of B cells in TACI-deficient mice. Nat. Immunol. *2*, 638–643.

Ye, Q., Wang, L., Wells, A.D., Tao, R., Han, R., Davidson, A., Scott, M.L., and Hancock, W.W. (2004). BAFF binding to T cell-expressed BAFF-R costimulates T cell proliferation and alloresponses. Eur. J. Immunol. *34*, 2750–2759.

Zhou, L., and Littman, D.R. (2009). Transcriptional regulatory networks in Th17 cell differentiation. Curr. Opin. Immunol. *21*, 146–152.

iScience, Volume *23*

Supplemental Information

TACI Constrains T_H17 Pathogenicity and Protects against Gut Inflammation

Andy Hee-Meng Tan, Gloria Hoi Wan Tso, Biyan Zhang, Pei-Yun Teo, Xijun Ou, Sze-Wai Ng, Alex Xing Fah Wong, Sean Jing Xiang Tan, Arleen Sanny, Susana Soo-Yeon Kim, Alison P. Lee, Shengli Xu, and Kong-Peng Lam

TRANSPARENT METHODS

Mice. TACI$^{-/-}$ mice (Yan et al., 2001) were a kind gift of Vishva Dixit (Genentech). C57BL/6 (Stock No: 000664), B6.SJL-CD45.1 (C57BL/6 congenic; Stock No: 002014), μMT (Stock No: 002288) and RAG1$^{-/-}$ (Stock No: 002216) mice were purchased from The Jackson Laboratory. TACI$^{-/-}$ mice were backcrossed to C57BL/6 background for at least 6 generations before use. TACI$^{-/-}$ and μMT mice were crossed to generate TACI$^{-/-}$ μMT mice. All mice were bred in our animal facilities and maintained under specific pathogen-free conditions. Experiments conducted with TACI$^{-/-}$ and WT (C57BL/6) or TACI$^{-/-}$ μMT and μMT mice used mice of the different genotypes bred separately to generate age-matched mice which were neither littermates nor co-housed together. Experiments with mice were conducted according to guidelines issued by the A*STAR Biological Resource Centre Institutional Animal Care and Use Committee (IACUC).

Cell isolation and flow cytometry. Single cell suspensions of Spl and LN of mice were prepared by standard methods. Single cells were isolated from PP and LP using a previously reported protocol (Couter and Surana, 2016) with some modifications. Before staining with relevant fluorochrome-conjugated Abs, cells were treated with F_c block (Ab against CD16/32, 93; eBioscience). Abs against CD4 (GK1.5), CD62L (MEL-14), CD44 (IM7), TACI (CD267; 8F10), IL-17A (TC11-18H10), IFN-γ (XMG1.2), IL-4 (11B11) and IL-10 (JES5-16E3) were from BD Biosciences. Abs against CD25 (PC61.5), RORγt (B2D) and Foxp3 (FJK-16s) were from eBioscience. Abs against CD3 (145-2C11), TCRβ (H57-597) and BAFF-R (CD268; 7H22-E16) were from Biolegend. Ab against BCMA (CD269; 161616) was from R&D Systems. BAFF tagged with mouse IgG2a Fc (BAF-M5257) was from

ACROBiosystems and APRIL tagged with human IgG Fc (PKSM041367) was from Elabscience. Secondary Abs against mouse IgG2a (m2a-15F8) and human IgG Fc were from eBioscience. Antibody 4',6-diamidino-2-phenylindole (DAPI; Sigma-Aldrich) or Zombie Aqua™ Fixable Viability Dye (BioLegend) was used to exclude dead cells. To perform intracellular staining of cytokines, $CD3^+CD4^+$ T cells were first stimulated with 50 ng/ml PMA and 1 μg/ml ionomycin (Sigma-Aldrich) at 37°C for 4 h and BD GolgiPlug™ (BD Biosciences) was added to the cultures in the last 2 h. Cells were then collected and stained with Abs against appropriate cell surface molecules, fixed and permeabilized with BD Cytofix/Cytoperm Kit (BD Biosciences) before staining with Abs against cytokines. Foxp3 / Transcription Factor Staining Buffer Set (eBioscience) was used for visualizing the expression of transcription factors RORγt and Foxp3 in $CD3^+CD4^+$ T cells *ex vivo*. Samples were acquired on a LSRII cytometer (BD Biosciences) and analyzed with FlowJo software (TreeStar).

Stimulation of $CD4^+$ T cells with cytokines and measurement of cytokine production by ELISA. WT and $TACI^{-/-}$ $CD3^+CD4^+$ T cells were grown in Iscove's Modified Dulbecco's Medium (IMDM) supplemented with 10% fetal bovine serum (FBS), L-glutamine, sodium pyruvate and penicillin/streptomycin (all from Sigma-Aldrich). Cells were activated by 1 μg/ml plate-bound anti-CD3 Ab and 1 μg/ml soluble anti-CD28 Ab and differentiated for 3 days into T_H0 (10 μg/ml anti-IFN-γ + 10 μg/ml anti-IL-4 Abs), T_H1 (10 ng/ml IL-12 + 10 μg/ml anti-IL-4 Ab), T_H2 (10 ng/ml IL-4 + 10 μg/ml anti-IFN-γ Ab), T_H17 (5 ng/ml TGF-β + 20 ng/ml IL-6 + 5 ng/ml IL-23) and T_{reg} (5 ng/ml TGF-β + 100 IU/ml IL-2) lineages *in vitro*. All Abs were obtained from eBioscience and all cytokines were from R&D Systems. In control experiments, B cells enriched from WT spleen were labeled with 1 μM CellTrace™ CFSE

(Invitrogen) and activated with 1 μg/ml LPS (Sigma) in the presence of vehicle or increasing concentrations (0.1, 1, 10, 100 ng/ml) of recombinant mouse BAFF or APRIL (both from R&D Systems) for 4 days, followed by flow cytometric assessment of CFSE dilution. In parallel, vehicle or increasing concentrations (as above) of either cytokine was added to T_H17 or T_{reg} cultures. To examine cytokine secretion by T_H cells differentiated *in vitro*, cells were harvested and counted on day 3. 5×10^5 cells were then re-seeded in fresh media and re-stimulated by 1 μg/ml plate-bound anti-CD3 Ab. 24 h later, culture supernatants were harvested to perform enzyme-linked immunosorbent assay (ELISA) using kits to detect mouse IFN-γ, IL-4 and IL-17A (Thermo FisherScientific). To determine if TACI deficiency affected TCRβ expression in $CD3^+CD4^+$ T cells, TCRβ expression in unstimulated WT and $TACI^{-/-}$ T cells or cells activated by 1 μg/ml plate-bound anti-CD3 Ab and 1 μg/ml soluble anti-CD28 Ab for 24 h were assessed.

Generation of bone marrow chimeras. 6 week-old female C57BL/6 mice were subjected to a dose of 900 cGy in a γ-irradiator at a rate of ~1Gy/min to deplete their hematopoietic compartments. 24 h later, BM cells were harvested from $CD45.1^+$ WT and $CD45.2^+$ $TACI^{-/-}$ mice, mixed in a 1:1 ratio (1×10^6 cells each) and injected intravenously into irradiated mice. The health of recipient mice was closely monitored and flow cytometric assessment of their blood lymphocytes 4 weeks post injection confirmed successful BM reconstitution and chimerism (data not shown). Chimeric mice between 8 to 10 weeks post injection were then sacrificed to analyse the frequencies and numbers of T_H17 and T_{reg} cells in various organs.

RNA isolation and quantitative real-time PCR. Total RNA was isolated using TRIzol (Thermo Fisher Scientific) and precipitated with isopropanol. cDNA was prepared using RevertAid H Minus First-Strand cDNA Synthesis Kit (Fermentas) and real-time PCR performed using SYBR Green Master Mix on the ABI Prism 7500 system (Applied Biosystems). Primer sequences were as follows: TACI forward, 5'-GAG CTC GGG AGA CCA CAG GCC-3'; TACI reverse, 5'-GGC AGA CCC CCA GTG TGC AGT A-3'; IRF4 forward, 5'-GCT GCA TAT CTG CCT GTA TTA CCG-3'; IRF4 reverse, 5'-GTG GTA ACG TGT TCA GGT AAC TCG TAG-3'; c-MAF forward, 5'-AGC AGT TGG TGA CCA TGT CG-3'; c-MAF reverse, 5'-TGG AGA TCT CCT GCT TGA GG-3'; JUNB forward, 5'-TCA CGA CGA CTC TTA CGC AG-3'; JUNB reverse, 5'-CCT TGA GAC CCC GAT AGG GA-3'; FOS forward, 5'-CGG GTT TCA ACG CCG ACT A-3'; FOS reverse, 5'-TTG GCA CTA GAG ACG GAC AGA-3'; EGR2 forward, 5'-CCT CCA CTC ACG CCA CTC TC-3'; EGR2 reverse, 5'-CAC CAC CTC CAC TTG CTC CTG-3'; SLC3A2 forward, 5'- GAA GAT CAA GGT GGC GGA GGA C-3'; SLC3A2 reverse, 5'- CAA GTA CTC CAG ATG GCT CTT CAG ACC-3'; AP-1/JUN forward, 5'-CCA GAA GAT GGT GTG GTG TTT-3'; AP-1/JUN reverse, 5'- CTG ACC CTC TCC CCT TGC-3'; GAPDH forward, 5′-TGT GTC CGT CGT GGA TCT GA-3′, GAPDH reverse, 5′-TTG CTG TTG AAG TCG CAG GAG-3′. Transcript levels of genes were normalized to those of GAPDH.

Western blotting. $CD4^{+}CD62L^{hi}CD44^{lo}CD25^{-}$ T_{naive} cells were FACS-sorted from pooled Spl and LN of $TACI^{-/-}$ or WT mice and stimulated or not for 4 h and 24 h with anti-CD3 and anti-CD28 Abs. In some experiments, T_{naive} cells were cultured for 24 h in T_H17-polarizing conditions with or without 100 ng/ml CsA. Cells were subsequently lysed using NE-PER™ Nuclear and Cytoplasmic Extraction Reagents (Thermo

Fisher Scientific) according to manufacturer's instructions to extract separate cytoplasmic and nuclear protein fractions. Protein concentrations were quantified by the bicinchoninicacid (BCA) assay (Pierce) and read in an Infinite® M1000 PRO microplate reader (TECAN). For Western blot analysis, equal amounts of proteins were separated by sodium dodecyl sulphate- polyacrylamide gel electrophoresis (SDS-PAGE), transferred onto a nitrocellulose membrane and blotted with specific Abs against NFAT1 (#5861), NFAT2 (#8032), NFAT4 (#4998), IRF4 (#4964) and JUNB (#3753) were obtained from Cell signalling. Abs against c-MAF (sc-7866) and HDAC1 (sc-8410) were purchased from Santa Cruz and Ab against RORγt (B2D) was from eBioscience.

Induction of colitis and evaluation of disease severity. To induce acute colitis, 2% (w/v) dextran sodium sulphate (DSS, molecular mass 36–50 kDa; Sigma-Aldrich) was added to drinking water and fed to mice *ad libitum* for up to 15 days. To induce chronic colitis, 5×10^5 $CD4^+CD62L^{hi}CD44^{lo}CD25^-$ T_{naive} or $CD4^+CD62L^{hi}CD44^{lo}CD25^+$ T_{reg} cells were FACS-sorted on a FACSAria III (BD Biosciences) from Spl and LN of $TACI^{-/-}$ or WT mice and T_{naive} cells alone or in conjunction with T_{reg} cells were intraperitoneally injected into age- and gender-matched $RAG1^{-/-}$ mice. For both acute and chronic colitis models, mice were observed for signs of colitis by monitoring weight loss, stool consistency and blood in the stool (data not shown for latter 2 parameters). Any animal showing clinical symptoms of debilitating disease (with weight loss > 30% of original weight) and became moribund were sacrificed following Institutional Animal Care and Use Committee regulations. The weight losses of such mice were not included in the generation of curves depicted in Figures 4A, 5A, 5E and 5G.

Colon histology. Entire colons were removed from mice 0 or 6 days after DSS treatment, cut open lengthwise, gently cleaned with sterile phosphate-buffered saline (PBS) to remove faeces and fixed in 10% neutral buffered formalin (NBF). 4 – 6 μm paraffin-embedded sections were cut and stained with hematoxylin and eosin (H&E), hematoxylin and Ki-67 (Abcam) or hematoxylin and periodic acid Schiff (Abcam). Histomorphological scoring of colon pathology was performed in a blinded fashion based on the criteria of severity and spatial extent of inflammation due to infiltration by immune cells, degree of epithelial cell loss and ulceration, hyperplasia and dysplasia as previously described (Erben et al., 2014).

Microarray analysis. T_{naive} cells were FACS-sorted from Spl and LN of WT and $TACI^{-/-}$ mice (n = 2 each). Total RNA was isolated using TRIzol (Invitrogen) and precipitated with isopropanol, followed by DNase I digestion using RNase-Free DNase Set and purification using RNeasy MinElute Cleanup Kit (both kits from Qiagen). After quantification with NanoDrop ND-2000 spectrophotometer and determination that the RNA integrity number (RIN) of all RNA samples were > 8.5 with Agilent 2100 Bioanalyzer, single-stranded cDNA was then prepared and hybridized on a GeneChip Mouse Gene 2.0 ST Array (Affymetrix). Significantly differentially expressed genes (DEGs) between $TACI^{-/-}$ and WT T_{naive} cells (fold change > 1.5-fold; two-tailed *t*-test with equal variances, $p < 0.05$) were detected using Partek Genomics Suite (PGS) software (Partek Inc.). GSEA was performed to identify the most significantly enriched gene sets corresponding to specific cellular and transcriptional pathways based on DEGs between $TACI^{-/-}$ vs WT T cells.

Calcium flux assay. $CD3^+CD4^+$ T cells were enriched from the Spl of WT and $TACI^{-/-}$ mice using Naive $CD4^+$ T Cell Isolation Kit, mouse as above and incubated with 4 μM Indo-1 acetoxy-methyl ester (Indo-1 AM, Molecular Probes) for 1 h at 37°C in complete media. Cells were then stained with anti-CD4 Ab, their density adjusted to 1×10^6 cells/ml and equilibrated for 10 min at room temperature. An initial 3 min baseline Indo-1 AM fluorescence reading was acquired on the LSRII before 15 μg/ml biotinylated anti-CD3 Ab and 100 μg/ml streptavidin were added. Calcium flux was measured in real time for a further 15 min and 2 μM ionomycin was then added to induce equivalent maximal fluxing from both WT and $TACI^{-/-}$ T cells as a positive control. Intracellular calcium concentration was calculated based on the ratio of fluorescence at 395 and 525 nm.

Statistical analyses. Differences in numerical values between samples were compared by unpaired *t*-test for parametric data sets with 2 variables, Mann-Whitney test for non-parametric data sets, two-way repeated-measures analysis of variance (ANOVA) and log-rank (Mantel-Cox) test respectively for colitis-associated weight loss data and Kaplan-Meier survival curves using Prism (version 8; GraphPad Software). In general, a value of $p < 0.05$ for a given comparison was regarded as statistically significant.

SUPPLEMENTAL REFERENCES

Couter, C.J., Surana, N.K., 2016. Isolation and flow cytometric characterization of murine small intestinal lymphocytes. J. Vis. Exp. 2016. https://doi.org/10.3791/54114

Erben, U., Loddenkemper, C., Doerfel, K., Spieckermann, S., Haller, D., Heimesaat, M.M., Zeitz, M., Siegmund, B., Ku¨hl, A.A., 2014. A guide to histomorphological evaluation of intestinal inflammation in mouse models. Int. J. Clin. Exp. Pathol. 7, 4557–4576.

Yan, M., Wang, H., Chan, B., Roose-Girma, M., Erickson, S., Baker, T., Tumas, D., Grewal, I.S., Dixit, V.M., 2001. Activation and accumulation of B cells in TACI-deficient mice. Nat. Immunol. 2, 638–643. https://doi.org/10.1038/89790

Figure S1. Expression of BAFF-R and BCMA in $CD4^+$ T cells stimulated under various T_H-polarizing conditions. Related to Figure 1. BAFF-R and BCMA expression in WT (blue histogram) and $TACI^{-/-}$ (red histogram) splenic $CD3^+CD4^+$ T cells stimulated under T_H0-, T_H1-, T_H2-, T_H17- or T_{reg}-polarizing conditions for 3 days as assessed by flow cytometry. Shaded histogram represents staining by isotype control Ab. Data are representative of 2 independent experiments.

Figure S2. TACI constrains production of IL-17A by T_H17 cells. Related to Figure 1. WT and $TACI^{-/-}$ $CD4^+$ T cells were differentiated under T_H0-, T_H1-, T_H2- or T_H17-polarizing conditions for 3 days as in Figures 1A, B and C, re-seeded in equal numbers and re-stimulated for further 1 day. The concentrations of IFN-γ **(A)**, IL-4 **(B)** and IL-17A **(C)** secreted in the culture supernatant by the different T_H lineages were then measured by ELISA. Cells were also separately differentiated under T_{reg}-polarizing conditions and their intracellular Foxp3 expression was assessed by flow cytometry **(D)**. Data in **(A to D)** are the mean ± SEM of 3 technical replicates; unpaired parametric *t*-test; **, $p < 0.01$; ****; $p < 0.0001$; ns, not significant. Actual *p*-

values are indicated in parentheses below the asterisks or “ns”. All data are representative of 2 independent experiments; n.d., not detected.

Figure S3. BAFF and APRIL neither bind CD4$^+$ T cells nor affect T_H17 or T_{reg} differentiation. Related to Figure 1. (A) B cells were enriched from WT spleen, labeled with CFSE and stimulated with LPS in the presence of empty vehicle (blue histogram) or increasing concentrations (1, 10 or 100 ng/ml) of BAFF or APRIL (red histograms) for 4 days, following which CFSE dilution was assessed by flow cytometry. Shaded histogram represents CFSE expression of unstimulated, labeled B cells. The mean frequencies of proliferated B cells stimulated with LPS in the presence of each BAFF or APRIL concentration, assessed from gating on diluted CFSE peaks, were compared with that of cells stimulated with LPS alone. **(B)** WT and TACI$^{-/-}$ CD4$^+$ T cells were differentiated under T_H17- or T_{reg}-polarizing conditions in the presence of vehicle or increasing concentrations of BAFF or APRIL as in **(A)** for 3 days, following which their expression of IL-17A (top panel) or Foxp3 (bottom panel) was assessed. **(C)** Flow cytometric assessment of binding of BAFF or APRIL to splenic B or CD4$^+$ T cells (blue histograms) compared with background binding due to secondary Ab alone (shaded histograms). All data are representative of 2 independent experiments. Data for bar plots in **(A)** are the mean ± SEM of at least 3 technical replicates; unpaired parametric *t*-test; **, $p < 0.01$; ns, not significant.

Figure S4. Gating strategies to identify T_H17 or T_{reg} cells in LP of $TACI^{-/-}$ and WT mice and in LP of BM chimeras. Related to Figures 2 and 3. Cells isolated from the LP of $TACI^{-/-}$ and WT mice were stimulated as in Figures 2A and B and assessed for intracellular IL-17A and IL-10 **(A)** or Foxp3 and RORγt **(B)** expression in $CD3^+CD4^+$ T cells by flow cytometry. **(C and D)** Cells isolated from LP of BM chimeric mice were stimulated and assessed as in **(A and B)**. Gating on live cells was followed by $CD45^+CD3^+CD4^+IL\text{-}17^+$ and $IL\text{-}10^+$ **(A)** or $Foxp3^+$ and $ROR\gamma t^+$ **(B)** cells. Similar strategies were applied in BM chimeras to analyze $IL\text{-}17^+$ and $IL\text{-}10^+$ **(C)** or $Foxp3^+$ and $ROR\gamma t^+$ **(D)** cells except that $TACI^{-/-}$ CD3+CD4+ T cells were distinguished by expression of CD45.2 from WT counterparts by expression of CD45.1. $IL\text{-}17^+$ and $Foxp3^+$ cells were used to respectively identify T_H17 and T_{reg} cells due to their more consistent expression between mouse replicates (Figures 2 and 3). Data in **(A and B)** are representative of at least 7 $TACI^{-/-}$ and WT mice and in **(C and D)** of at least 11 BM chimeras.

Figure S5. Gating strategies utilizing relevant no staining controls to identify T_H17 or T_{reg} cells in $TACI^{-/-}$ and WT mice. Related to Figure 2. Cells isolated from various indicated organs of $TACI^{-/-}$ and WT mice were stimulated as in Figures 2A and B and assessed for intracellular IL-17A and IL-10 **(A)** or Foxp3 and RORγt **(B)** expression in $CD3^+CD4^+$ T cells by flow cytometry. Gating on live cells was followed by $CD45^+CD3^+CD4^+IL\text{-}17^+$ and $IL\text{-}10^+$ (A) or $Foxp3^+$ and $ROR\gamma t^+$ (B) cells. Relevant no staining controls for $IL\text{-}17A^+$, $IL\text{-}10^+$, $ROR\gamma t^+$ and $Foxp3^+$ cells amongst $CD3^+CD4^+$ T cells of $TACI^{-/-}$ vs WT mice were included to clearly separate cells which expressed a certain cytokine or transcription factor from those that did not. Data are representative of at least 7 $TACI^{-/-}$ and WT mice.

Figure S6. Gating strategies utilizing relevant no staining controls to identify T_H17 or T_{reg} cells amongst $TACI^{-/-}$ and WT $CD3^+CD4^+$ T cells in BM chimeric mice. Related to Figure 3. Cells isolated from various indicated organs of BM chimeric mice were stimulated as in Figures 2A and B and assessed for intracellular IL-17A and IL-10 **(A)** or Foxp3 and RORγt **(B)** expression amongst $TACI^{-/-}$ ($CD45.2^+$) and WT ($CD45.1^+$) $CD3^+CD4^+$ T cells by flow cytometry. As in Figure S4, relevant no staining controls for $IL\text{-}17A^+$, $IL\text{-}10^+$, $ROR\gamma t^+$ and $Foxp3^+$ cells amongst $TACI^{-/-}$ ($CD45.2^+$) and WT ($CD45.1^+$) $CD3^+CD4^+$ T cells were included to clearly separate cells which expressed a certain cytokine or transcription factor from those that did not. Data are representative of at least 11 BM chimeras.

Figure S7. Normal frequencies and numbers of T_H1 and T_H2 cells in $TACI^{-/-}$ mice. Related to Figure 2. Cells from the Spl and mLN of $TACI^{-/-}$ (filled circles) or WT (open circles) mice were stimulated as in Figures 2A and B. Frequencies and numbers of $CD3^+CD4^+$ T cells expressing IFN-γ **(A and B)** or IL-4 **(C and D)** was assessed by flow cytometry. Data in **(A and C)** are representative of 4 mice of each genotype analyzed. Data in **(B and D)** are based on 4 mice analyzed with each symbol representing one mouse and horizontal bars indicating the mean; Mann-Whitney test, ns, not significant.

Figure S8. RORγt upregulation in WT and $TACI^{-/-}$ T_{naive} cells induced by T_H17-polarizing conditions is attenuated by CsA treatment. Related to Figure 6. Flow cytometry analysis of RORγt expression in WT and $TACI^{-/-}$ T_{naive} cells activated under T_H17-polarizing conditions in the presence or absence of CsA for 24 h as in Figure 6E. Data are representative of 2 independent experiments.

Figure S9. TCRβ expression in TACI$^{-/-}$ and WT CD4^{+} T cells. Related to Figure 6.

TCRβ expression in CD4^{+} T cells from the Spls of WT (blue histogram) and TACI$^{-/-}$ (red histogram) mice left unstimulated or stimulated with plate-bound anti-CD3 and soluble anti-CD28 Abs for 24 h as assessed by flow cytometry. Shaded histogram represents staining by isotype control Ab. Data are representative of 2 independent experiments.

Figure S1

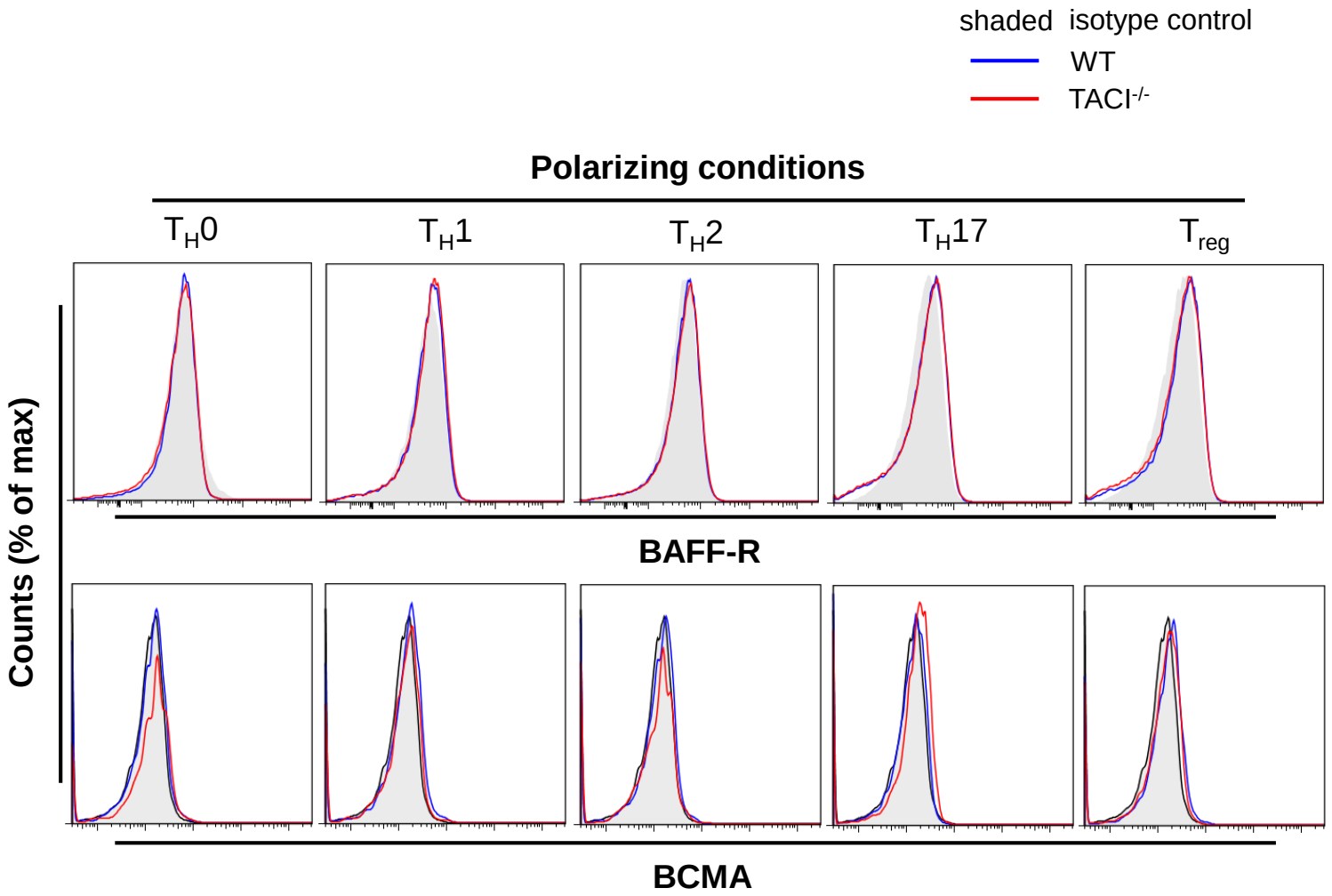
shaded isotype control
WT
TACI-/-
Polarizing conditions
TH0
TH1
TH2
TH17
Treg
Counts (% of max)
BAFF-R
BCMA

Figure S2

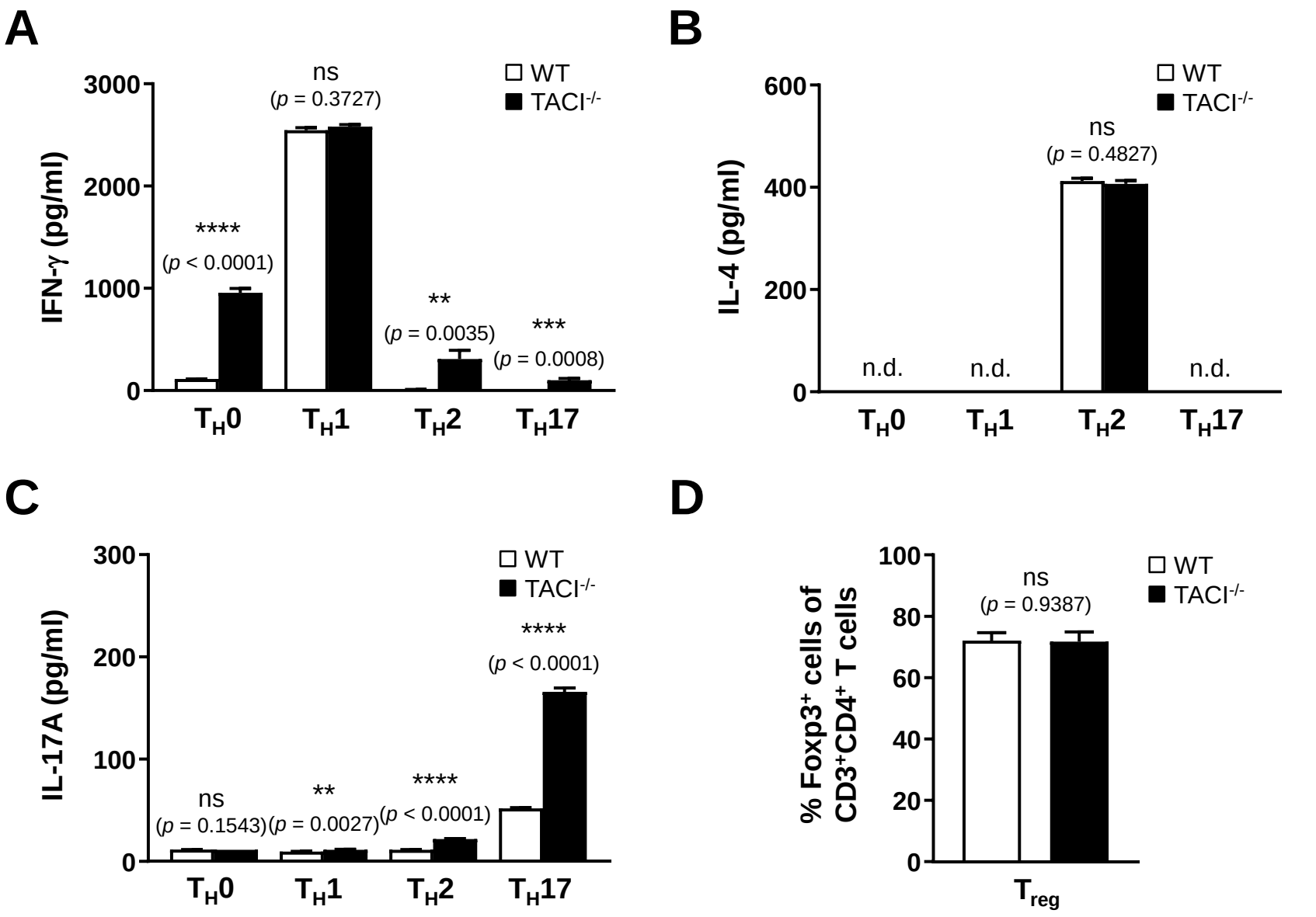
A
IFN-γ (pg/ml)
3000
2000
1000
0
WT
TACI-/-
ns
(p = 0.3727)
****
(p < 0.0001)
**
(p = 0.0035)
***
(p = 0.0008)
TH0
TH1
TH2
TH17
B
IL-4 (pg/ml)
600
400
200
0
WT
TACI-/-
ns
(p = 0.4827)
n.d.
n.d.
n.d.
TH0
TH1
TH2
TH17
C
IL-17A (pg/ml)
300
200
100
0
WT
TACI-/-
ns
(p = 0.1543)
**
(p = 0.0027)
****
(p < 0.0001)
****
(p < 0.0001)
TH0
TH1
TH2
TH17
D
% Foxp3+ cells of CD3+CD4+ T cells
100
80
60
40
20
0
WT
TACI-/-
ns
(p = 0.9387)
Treg

Figure S3

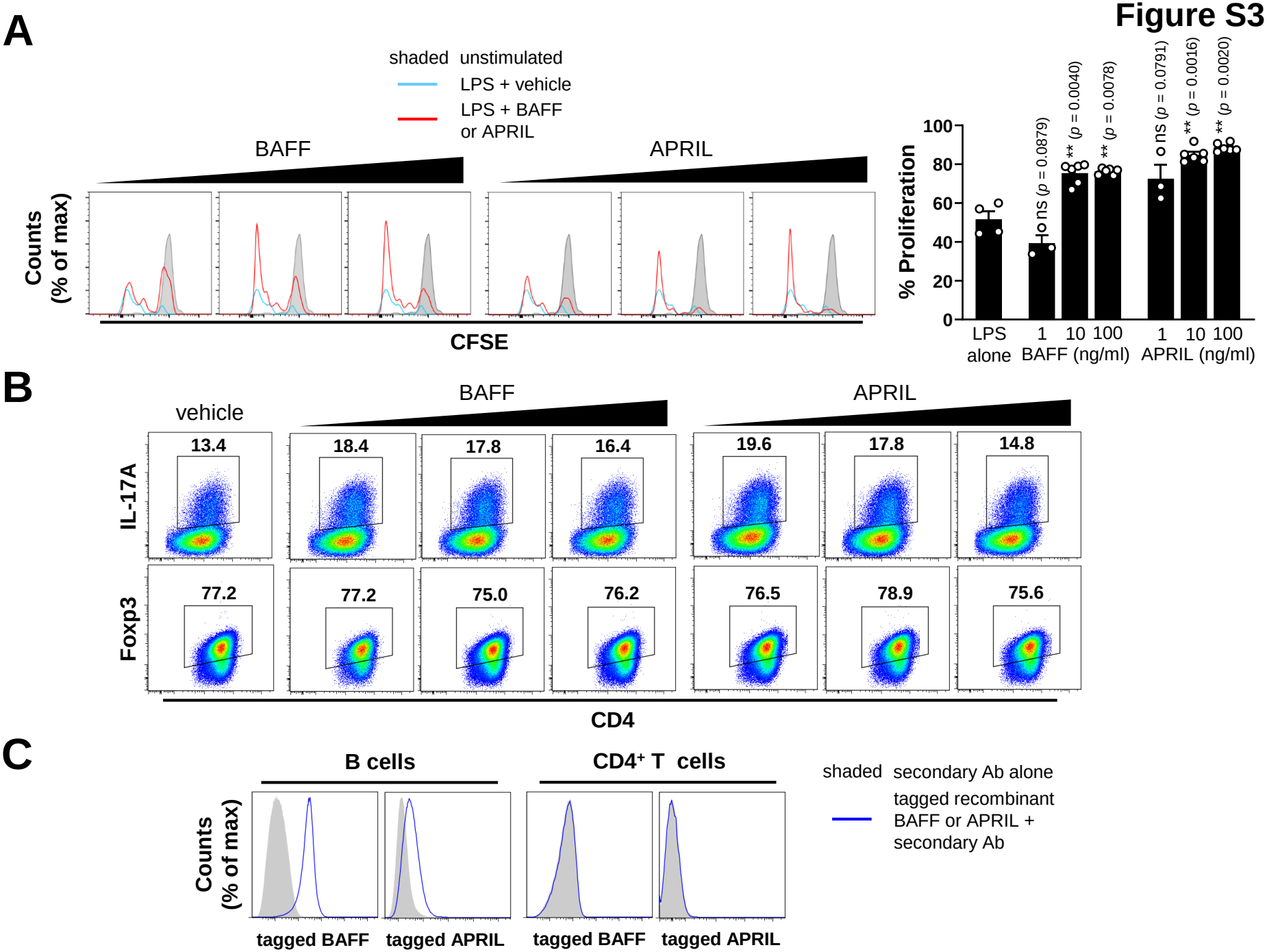
A
shaded unstimulated
LPS + vehicle
LPS + BAFF or APRIL
BAFF
APRIL
Counts (% of max)
CFSE
% Proliferation
ns (p = 0.0879)
** (p = 0.0040)
** (p = 0.0078)
ns (p = 0.0791)
** (p = 0.0016)
** (p = 0.0020)
LPS alone
1
10
100
BAFF (ng/ml)
APRIL (ng/ml)
B
vehicle
BAFF
APRIL
IL-17A
Foxp3
13.4
18.4
17.8
16.4
19.6
17.8
14.8
77.2
77.2
75.0
76.2
76.5
78.9
75.6
CD4
C
B cells
CD4+ T cells
Counts (% of max)
tagged BAFF
tagged APRIL
tagged BAFF
tagged APRIL
shaded secondary Ab alone
tagged recombinant BAFF or APRIL + secondary Ab

Figure S4

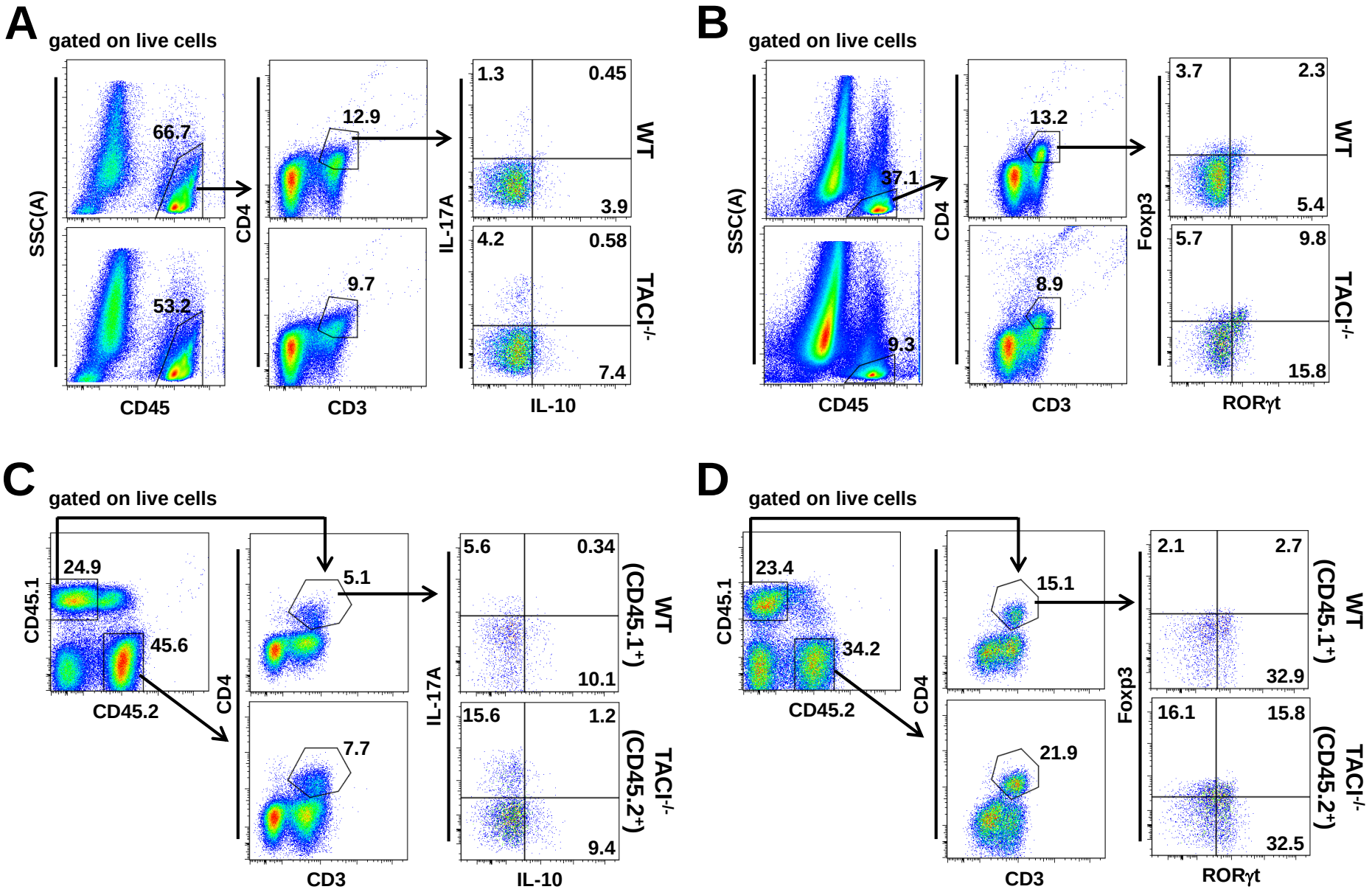
A
gated on live cells
SSC(A)
CD45
66.7
53.2
CD4
CD3
12.9
9.7
IL-17A
IL-10
1.3
0.45
3.9
4.2
0.58
7.4
WT
TACI-/-
B
gated on live cells
SSC(A)
CD45
37.1
9.3
CD4
CD3
13.2
8.9
Foxp3
RORγt
3.7
2.3
5.4
5.7
9.8
15.8
WT
TACI-/-
C
gated on live cells
CD45.1
CD45.2
24.9
45.6
CD4
CD3
5.1
7.7
IL-17A
IL-10
5.6
0.34
10.1
15.6
1.2
9.4
WT (CD45.1+)
TACI-/- (CD45.2+)
D
gated on live cells
CD45.1
CD45.2
23.4
34.2
CD4
CD3
15.1
21.9
Foxp3
RORγt
2.1
2.7
32.9
16.1
15.8
32.5
WT (CD45.1+)
TACI-/- (CD45.2+)

Figure S5

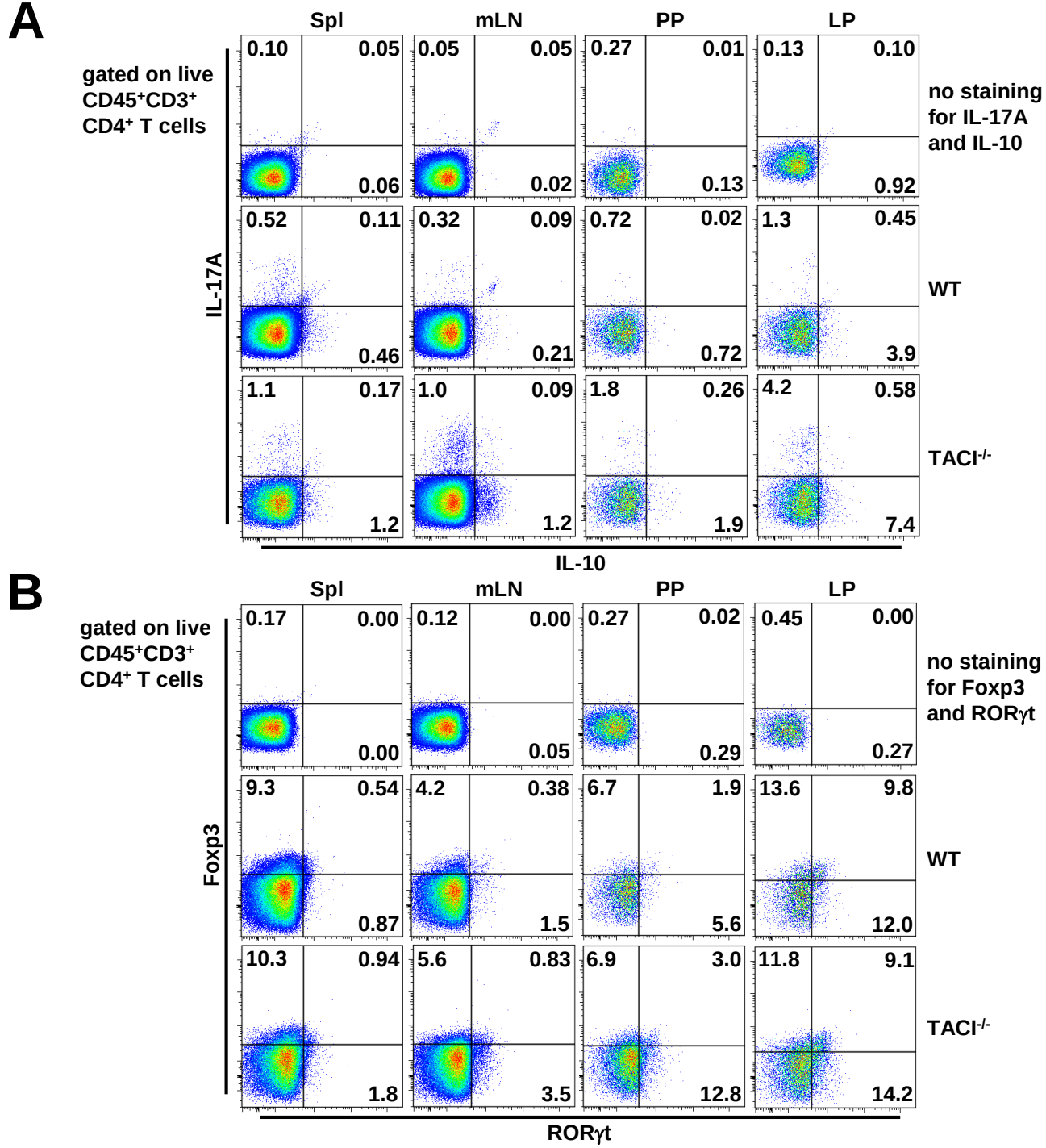
A
Spl
mLN
PP
LP
gated on live
CD45+CD3+
CD4+ T cells
no staining
for IL-17A
and IL-10
WT
TACI-/-
IL-17A
IL-10
0.10
0.05
0.06
0.05
0.05
0.02
0.27
0.01
0.13
0.13
0.10
0.92
0.52
0.11
0.46
0.32
0.09
0.21
0.72
0.02
0.72
1.3
0.45
3.9
1.1
0.17
1.2
1.0
0.09
1.2
1.8
0.26
1.9
4.2
0.58
7.4
B
Spl
mLN
PP
LP
gated on live
CD45+CD3+
CD4+ T cells
no staining
for Foxp3
and RORγt
WT
TACI-/-
Foxp3
RORγt
0.17
0.00
0.00
0.12
0.00
0.05
0.27
0.02
0.29
0.45
0.00
0.27
9.3
0.54
0.87
4.2
0.38
1.5
6.7
1.9
5.6
13.6
9.8
12.0
10.3
0.94
1.8
5.6
0.83
3.5
6.9
3.0
12.8
11.8
9.1
14.2

Figure S6

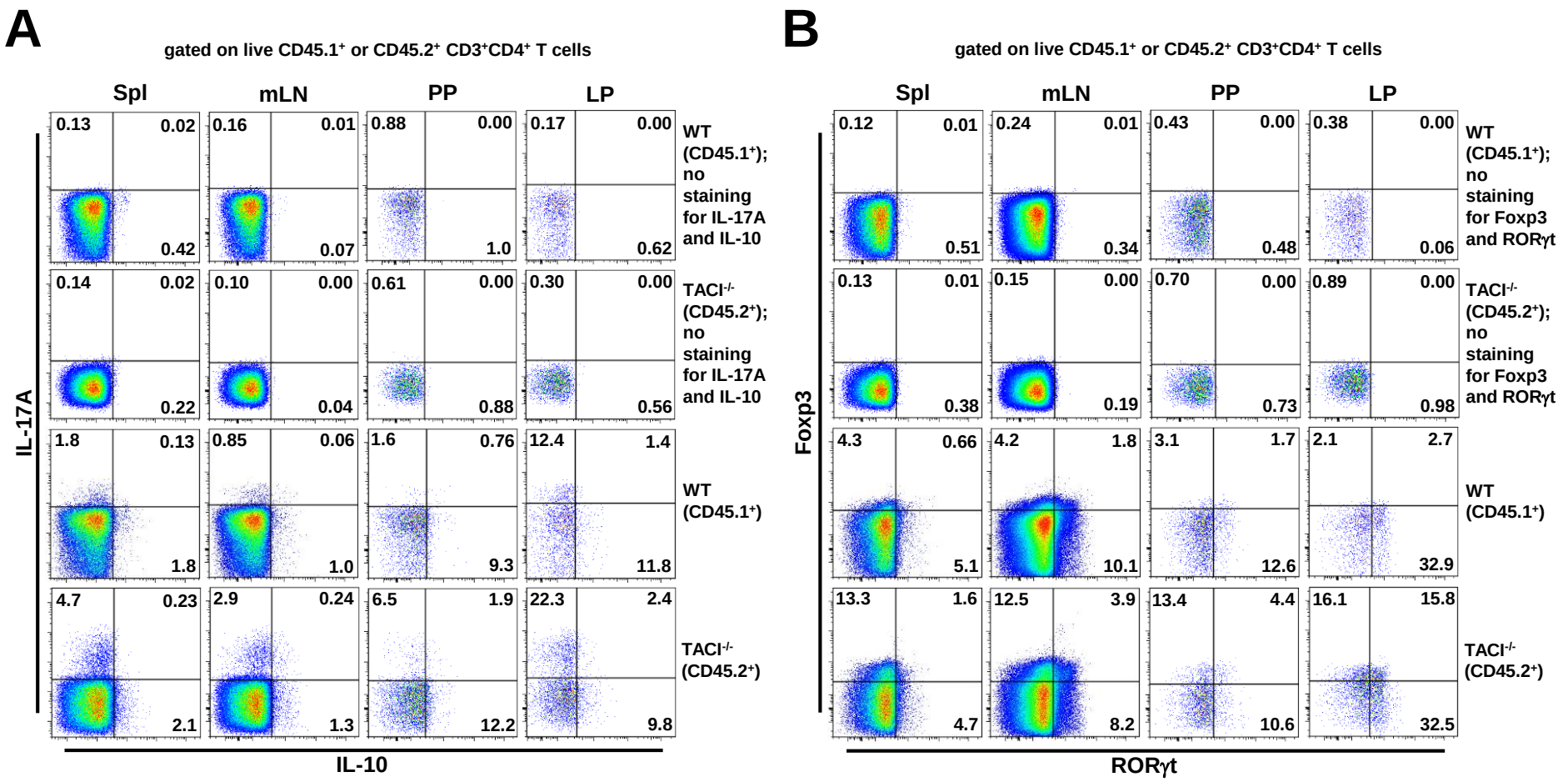
A
gated on live CD45.1+ or CD45.2+ CD3+CD4+ T cells
Spl
mLN
PP
LP
IL-17A
IL-10
0.13 0.02 0.42
0.16 0.01 0.07
0.88 0.00 1.0
0.17 0.00 0.62
WT (CD45.1+); no staining for IL-17A and IL-10
0.14 0.02 0.22
0.10 0.00 0.04
0.61 0.00 0.88
0.30 0.00 0.56
TACI-/- (CD45.2+); no staining for IL-17A and IL-10
1.8 0.13 1.8
0.85 0.06 1.0
1.6 0.76 9.3
12.4 1.4 11.8
WT (CD45.1+)
4.7 0.23 2.1
2.9 0.24 1.3
6.5 1.9 12.2
22.3 2.4 9.8
TACI-/- (CD45.2+)
B
gated on live CD45.1+ or CD45.2+ CD3+CD4+ T cells
Spl
mLN
PP
LP
Foxp3
RORγt
0.12 0.01 0.51
0.24 0.01 0.34
0.43 0.00 0.48
0.38 0.00 0.06
WT (CD45.1+); no staining for Foxp3 and RORγt
0.13 0.01 0.38
0.15 0.00 0.19
0.70 0.00 0.73
0.89 0.00 0.98
TACI-/- (CD45.2+); no staining for Foxp3 and RORγt
4.3 0.66 5.1
4.2 1.8 10.1
3.1 1.7 12.6
2.1 2.7 32.9
WT (CD45.1+)
13.3 1.6 4.7
12.5 3.9 8.2
13.4 4.4 10.6
16.1 15.8 32.5
TACI-/- (CD45.2+)

Figure S7

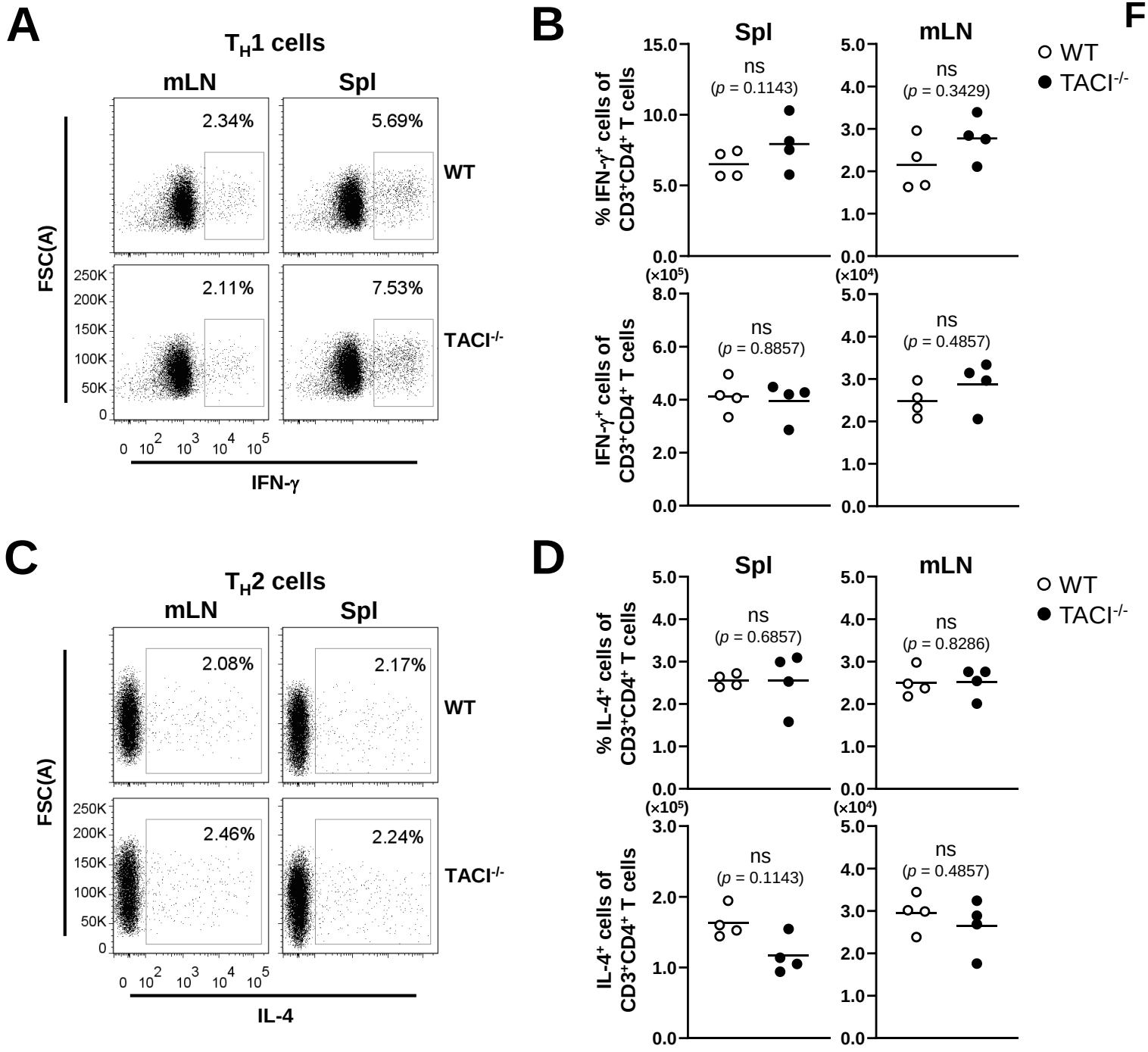
A
T_H1 cells
mLN
Spl
2.34%
5.69%
2.11%
7.53%
WT
TACI-/-
FSC(A)
IFN-γ
B
Spl
mLN
ns
(p = 0.1143)
ns
(p = 0.3429)
ns
(p = 0.8857)
ns
(p = 0.4857)
% IFN-γ+ cells of CD3+CD4+ T cells
IFN-γ+ cells of CD3+CD4+ T cells
(×10⁵)
(×10⁴)
WT
TACI-/-
C
T_H2 cells
2.08%
2.17%
2.46%
2.24%
IL-4
D
ns
(p = 0.6857)
ns
(p = 0.8286)
ns
(p = 0.1143)
ns
(p = 0.4857)
% IL-4+ cells of CD3+CD4+ T cells
IL-4+ cells of CD3+CD4+ T cells

Figure S8

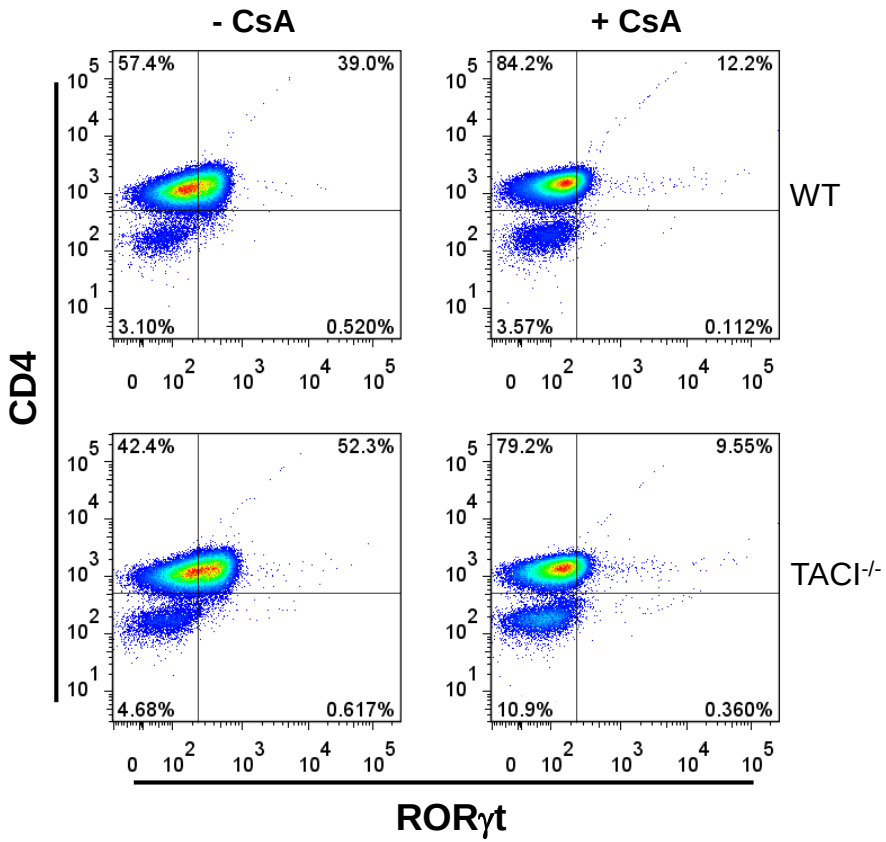
- CsA
+ CsA
57.4%
39.0%
3.10%
0.520%
84.2%
12.2%
3.57%
0.112%
42.4%
52.3%
4.68%
0.617%
79.2%
9.55%
10.9%
0.360%
WT
TACI-/-
CD4
RORγt

Figure S9

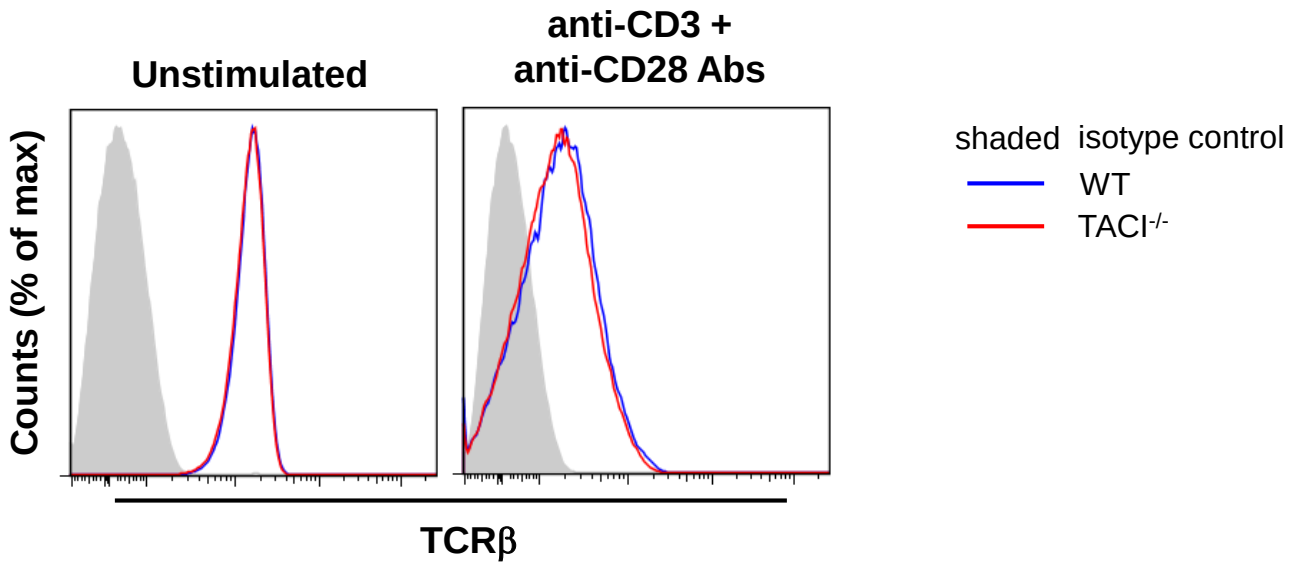
Unstimulated
anti-CD3 +
anti-CD28 Abs
Counts (% of max)
TCRβ
shaded isotype control
WT
TACI-/-